Microbial signatures in peritidal siliciclastic sediments: a catalogue

GISELA GERDES*, THOMAS KLENKE† and NORA NOFFKE*
*Carl von Ossietzky University of Oldenburg, ICBM Marine Laboratory, Schleusenstraße 1,
D-26382 Wilhelmshaven, Germany (E-mail: g.gerdes@icbm.terramare.de)
†Carl von Ossietzky University of Oldenburg, Institute for Chemistry and Biology of the Marine
Environment (ICBM), PO BOX 2503, D-26111 Oldenburg, Germany
(E-mail: klenke@icbm.de)*

ABSTRACT

A catalogue of microbial structural signatures is presented, based upon the coupling of fundamental biogeochemical–microbial processes and local morphogenetic determinants. It summarizes a collection of sedimentary structures obtained from two modern siliciclastic peritidal environments in different climatic zones (temperate humid: Mellum Island, southern North Sea; subtropical arid: coast of southern Tunisia). Textural geometries reveal a high structural diversity, but their determinants are primarily based upon six major parameters: (1) intrinsic biofactors: structural diversification of sedimentary microbial films and mats inherent in the organisms, i.e. their construction morphology, growth, taxis and behaviour, and local abundance of specific morphotypes. Most prominent are the ensheathed filamentous cyanobacteria *Microcoleus chthonoplastes* and *Lyngbya aestuarii*, and the sheathless filamentous cyanobacterium *Oscillatoria limosa*. (2) Biological response to physical disturbances: sediment supply, erosion and fracturing of surface layers resulting from desiccation cause growth responses of biofilms and microbial mats. (3) Trapping/binding effects: physicobiological processes give rise to grain orientations and wavy to lenticular lamina, lamina-specific grain arrangements and 'sucrose' calcium carbonate accumulations. (4) Secondary physical deformation of biogenic build-ups: mechanical stresses acting upon sediments overgrown and biostabilized by biofilms and mats produce erosional and overthrust structures. (5) Post-burial processes: textural fabrics that evolve from mechanical effects of gas formation from decaying mats, and features related to the formation of authigenic minerals (calcium carbonates, calcium sulphates, pyrite). (6) Bioturbation and grazing: post-depositional structures, such as *Skolithos*-type dwellings, traces of burrowing insects, gastropod grazing traces and faecal pellets. In synopsis, the catalogue firstly comprises a sound set of ubiquitous signatures. This uniformity in architectural characteristics is attributed to the presence and local dominance of certain microbes throughout the different settings. The catalogue secondly documents signatures that are extremely sensitive to tidal position, hydrodynamic regime and overall climatic conditions. These kinds of signature indicate narrow facies zones, which often coincide with the activity or dominance zones of certain organisms. An overview of structures of microbial origin from the fossil record underlines the potential of many of the signatures included in this catalogue to become fossilized and provide strong indicators of former siliciclastic tidal settings.

This article is in commemoration of Hans-Erich Reineck.

Keywords Biofilms, biostabilization, condensed fibrillar meshworks, microbial mats, sedimentary structures, thrombolitic fabrics.

INTRODUCTION

The upper intertidal and lower supratidal zones are characterized by a high degree of environmental fluctuation. Benthic photosynthetic microbes are commonly abundant in this area. Eurytopic cyanobacteria and diatoms initiate highly productive microbial ecosystems, in which externally fluctuating conditions of the environment are mitigated through the capacity of these organisms to produce water-retaining slime, to store energy by light-harvesting systems and to transform and transfer nutrients in biogeochemical cycles. Cyanobacteria establish layered accretions of biomass, thereby making a great contribution to the sediments and sedimentary structures.

Sedimentary structures formed by an interplay between microbial and physical processes are known from a variety of modern siliciclastic tidal flats. Such structures reveal geometric forms that appear to be different from primary physical structures; these include inhomogeneously cracked, sometimes upfolded margins of desiccation cracks, domed, pustular, rugose and crinkled surfaces, sharply projecting remains of partially eroded sedimentary surfaces, erosion pockets and folding like tablecloths (Reineck, 1979; Gerdes & Krumbein, 1987; Reineck *et al.*, 1990; Gerdes *et al.*, 1991, 1993, 1994a,b; Noffke *et al.*, 1996, 1997a,b). These structures may be difficult to preserve in siliciclastic sediments. On the other hand, several groups of 'problematic' sedimentary structures, which are extremely common in latest Proterozoic and Cambrian strata (e.g. wrinkle marks, Kinneyia ripples, 'elephant skin', sand chips), suggest microbial mediation (Gehling, 1991; Pflüger & Gresse, 1996; Hagadorn & Bottjer, 1997).

Microbial primary production involved in the development of peritidal sedimentary structures usually occurs at two basic levels: (1) compact microbial layers project above the siliciclastic sediment (microbial 'biostrome' type; see Glossary); (2) microbial films adhere closely to sand/silt grains and establish cohesive clastic layers. The development of one or the other design depends on both the dominance of different taxa and the different stages of maturity (Neu, 1994). Differentiation between compact microbial mats and clastic-enriched biofilms is necessary for the

purpose of facies diagnosis. Biofilms often represent initial stages of microbial mat successions. Monty (1976) also emphasized hierarchical ranks between 'cryptalgal fabrics' and microbial biostromes/bioherms.

Various features of microbial activity have been identified in peritidal settings, including smooth, tufted, pinnacle- and pincushion-like, blistered, pustular forms, benthic ooids and oncoids, aggregate grains, thrombolites and fenestrae (Bauld, 1984; Guerrero & Mas, 1989; Skyring & Bauld, 1990; Riding, 1991; Golubic & Knoll, 1993). Many of these structures show a wide range of distribution in different sedimentary environments; others are specific to a certain type of setting. A classification of morphogenetic types, taking into account the interaction between intrinsic biofactors (see Glossary) and physical forces, may be advantageous for the interpretation of depositional environments.

In this paper, studies from two siliciclastic peritidal environments in different climatic zones (temperate humid and subtropical arid) reveal some fundamental controls on sedimentary structures. First, both basic types, microbial biostromes and biofilms, occur at almost the same littoral position and, secondly, there are similar biogeochemical–microbial processes and even some of the same taxa involved. On the other hand, physical and physicochemical mechanisms (e.g. rates of sedimentation and burial, erosion, evaporation and desiccation) operate differently in the different settings studied.

The objective of this paper is to present a catalogue of sedimentary structures based upon the coupling of both fundamental and local morphogenetic controls. Knowledge of such coupling is of great importance for the interpretation of analogous sedimentary structures in the geological record. By way of cataloguing these structures, an overview of the phenotypical variability of structures is presented that may occur in similar facies associations.

STUDY SITES

Sedimentary structures have been studied from siliciclastic peritidal settings in the southern

North Sea and southern Tunisian coastal areas (Fig. 1).

Climatic, topographic and hydrographic conditions

The southern North Sea coast has a temperate, humid climate. Low atmospheric pressures, westerly winds and relatively high rates of rainfall are
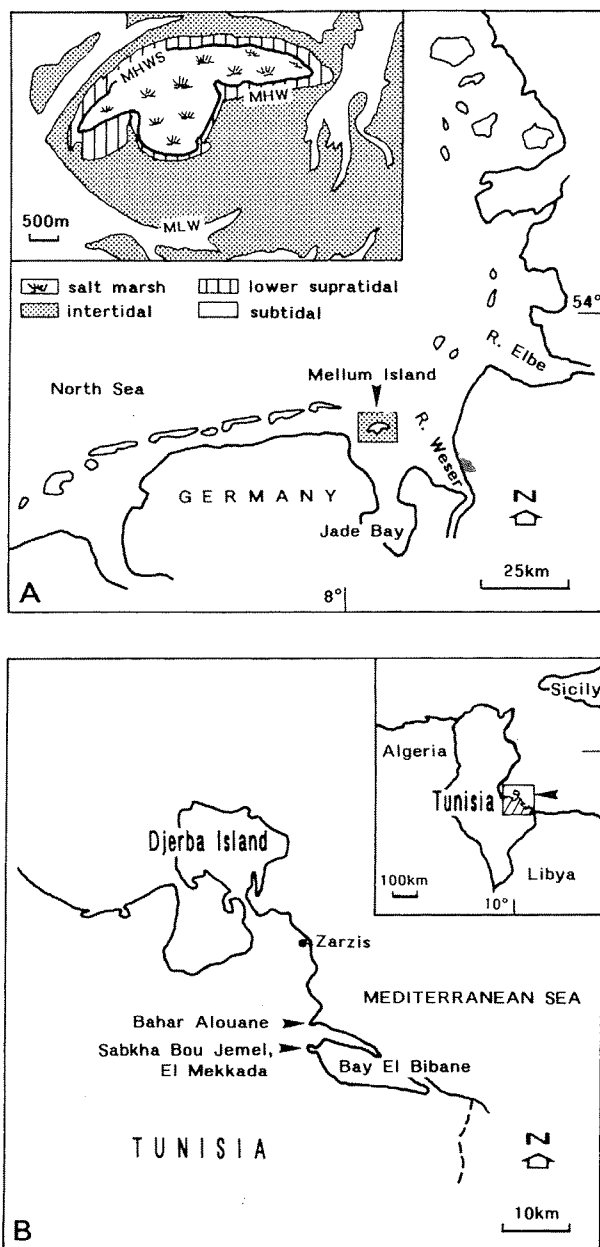

Fig. 1. Study localities. (A) Mellum Island, southern North Sea, geographical position and schematic view of back-barrier intertidal and supratidal zone. (B) Southern Tunisian coastal areas; arrows indicating study localities at Bahar Alouane and Sabkha Bou Jemel.

typical. Precipitation averages 700–750 mm per year. The tide is semi-diurnal. On high-lying sand flats along the coast, benthic cyanobacteria and diatoms fix and bind the sediments. Data for this study come primarily from Mellum Island (Fig. 1A), a sand bank situated in the Jade–Weser estuary, consisting of a complex of large sand flats in the intertidal, lower and upper supratidal range. The mean tidal range is 2·9 m, and the mean spring tidal range is 3·6 m. On a yearly average, more than 70% of the tides reach or cross the mean high water (MHW) level. Wind also influences the water level. Strong north-westerly winds raise it up to several metres above normal high-water level. Winds from the east or south may lower the water level. Thus, the energy regime driving transport pathways is controlled by a specific interplay of tide- and weather-related processes. Salinities range from 28‰ to 32‰. Sediments consist of about 95 wt% fine to medium quartz sand.

The southern Tunisian coast has a subtropical, semi-arid climate. Characteristic morphological features include lagoonal basins partially closed by coastal spits (Fig. 1B). Open marine waters are delivered to the lagoon via more or less narrow channels. Tides are in the microtidal range. In the barrier-island system of Jerba, north of the study area, the tidal range is up to 1·5 m during spring tides and winter storms (Davaud & Septfontaine, 1995). Cerithid gastropods live in the narrow intertidal zone of the lagoons. The lagoons are fringed by wide coastal sabkhas. The horizontal distribution of surface sea water results in a characteristic sequence of increasing salinity from the lagoon towards the higher lying sabkha [measurements during the study revealed a range from 40‰ (lagoon) to 180‰ (further inland sites of microbial mat growth). The sabkha sediments consist mainly of terrigenous siliciclastic material. Gypsum crystals form at the surface as well as within the sediments. Subsurface, chicken-wire anhydrite is common in the inner parts of the sabkhas.

Littoral positions of biofilm and mat formation

Mellum Island

Main occurrences of microbial films and mats are in the intertidal and lower supratidal range (Fig. 2, littoral positions I–III). The areas closely related to the diurnal tidal cycle are covered by initial stages of mat and biofilm development (Table 1). Dominant species are *Merismopedia*
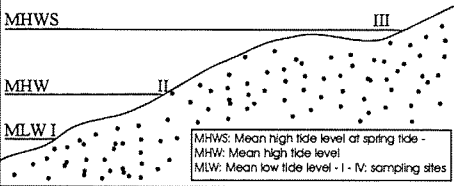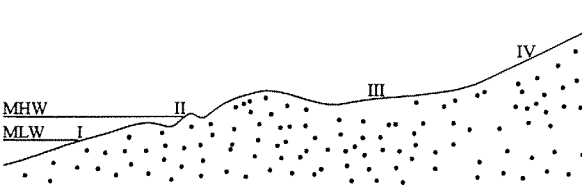
GEOGRAPHY	Southern North Sea			Southern Tunisian coast			
Locality	Mellum Island back-barrier intertidal and supratidal flats			Lagoon margins and sabkhas at Bahar Alouane and Bou Jemel			
Microbial environments							
Littoral positions	lower to middle intertidal zone	middle to upper intertidal zone	lower supratidal zone (shallows)	lagoon, subtidal to intertidal transition	lagoon, intertidal to supratidal transition	lower supratidal zone (shallows)	middle supratidal zone (sabkha)
Stages of mat development	initial (biofilms)	initial (biofilms)	fully developed	initial (biofilms)	fully developed	fully developed	initial (biofilms)
Positions of growth	cryptic (adhered to sand grains)	cryptic (mainly adhered to sand grains)	overgrowing the siliciclastic substrate	cryptic (adhered to sand grains)	overgrowing the inorganic substrate	overgrowing the inorganic substrate	cryptic (adhered to sand grains and evaporite crystals)
Tidal amplitude	meso- to macrotides: 2.90 m (mean tide), 3.60 m (spring tide)			microtide: 1.50 m (spring tide and storms)			
Effects of tidal flushing on the benthic systems	large			low			
Salinity	polyhaline to marine: 30-36 ‰			metahaline to hypersaline: 36-120 ‰			
Sedimentation (type, source)	siliciclastic quartz sands, marine			siliciclastic quartz sands (terrigenous-fluvial), clay (terrigenous-sheetfloods), detrital carbonates (marine), oolitic sands (marine), evaporites (*in situ*)			

Fig. 2. Comparative summary on environmental conditions in the study areas.

punctata and *Oscillatoria limosa* (Stal & Krumbein, 1985). These species predominantly adhere to sand grains. Slime-embedded bacterial cells and filaments cause grains to become agglutinated and stabilized against erosion. In vertical sections, thin cohesive layers of biomass appear containing relatively high quantities of mineral grains (Fig. 3A). Conditions in the lower supratidal zone support the development of mature perennial mats. The dominant mat builder is *Microcoleus chthonoplastes*. This species builds vertical accretions of organic matter that protrude above the siliciclastic substrate. Individual units are made of condensed fibrillar meshworks that contain relatively low quantities of mineral grains (Fig. 3B). High biomass production and successful surface sealing provided by the mats favours the development of versicoloured sand flats ('Farbstreifen-Sandwatt', Schulz, 1937). The term is related to the colourful vertical zonation of sedimentary layers resulting from: (1) blue–green cyanobacteria (top); (2) purple-coloured phototrophic sulphur bacteria (intermediate); and
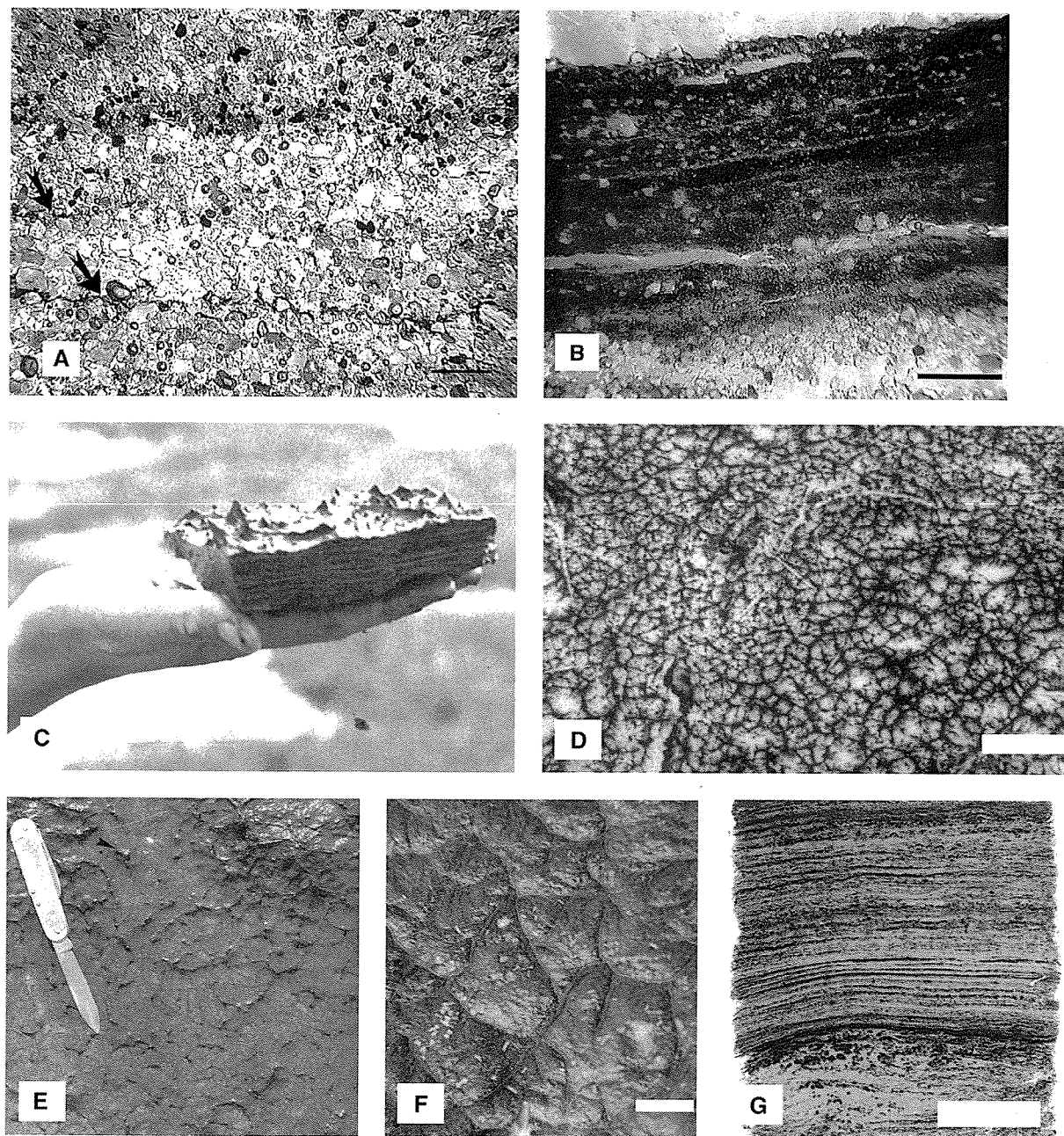
(3) black iron sulphide caused by the activity of sulphate-reducing bacteria (base).

Tunisian study sites

Microbial films and mats cover the lagoonal margins, lower supratidal shallows and parts of the higher lying sabkhas (Fig. 2, littoral positions I–IV). Lagoonal margins commonly display characteristic terraced outcrops that may result from the action of waves. On the lower terraces (littoral position I), cyanobacteria and diatoms agglutinate the fine-grained sediments with thin gel-supported films (Table 1). On the higher lying terraces (II), loaf-shaped hydroplastic cushions occur as a result of the dominance of coccoidal cyanobacteria that produce large amounts of extracellular polymeric substances (EPS). These build-ups contain relatively low amounts of sediment and completely mask the inorganic substrate. Between the lagoon margins and upper evaporitic plains, temporary higher water stands of the lagoons and high groundwater tables supply sea

Table 1. Major taxa and species diversity of biofilms and mats from the study areas.

Littoral positions (see Fig. 2)	Taxa	Species diversity	Biofacies (see Fig. 4)
Mellum Island			
I. Lower to middle intertidal zone	<u>Merismopedia punctata</u>, *Oscillatoria limosa, Phormidium* sp., diatoms (various species)	Low	Cohesive sand layers
II. Middle to upper intertidal zone	<u>Oscillatoria limosa</u>, *Merismopedia limosa, Chroococcus turgidus, Phormidium* spp., *Microcoleus chthonoplastes, Spirulina subsalsa*, diatoms (various species)	Medium	Cohesive sand layers
III. Lower supratidal zone	<u>Microcoleus chthonoplastes</u>, *Oscillatoria limosa, Merismopedia punctata, Chroococcus turgidus, Spirulina subsalsa, Phormidium* spp., *Nodularia* spp., diatoms (various species), anoxygenic phototrophic bacteria (various species)	High	Condensed fibrillar meshworks
Tunisian study sites			
I. Lagoon, subtidal to intertidal transition	Diatoms (various species), *Aphanothece* spp., *Phormidium* spp.	Low	Cohesive sand layers
II. Lagoon, intertidal to supratidal transition	<u>Aphanothece spp.</u>, *Entophysalis granulosa*, Pleurocapsalean species, *Phormidium* spp., *Lyngbya aestuarii* (rare), diatoms (rare)	Medium	Thrombolitic fabrics
III. Lower supratidal shallows	<u>Microcoleus chthonoplastes</u>, *Lyngbya aestuarii, Phormidium* spp., *Aphanothece* spp., *Entophysalis granulosa*, Pleurocapsalean species, *Spirulina* spp., *Gloeothece* sp., diatoms (various species)	High	Condensed fibrillar mesh works, biovarvites
IV. Middle supratidal zone, sabkha	*Entophysalis granulosa*, Pleurocapsalean species	Low	Cohesive sand/evaporite layers

Double underlinings, locally dominant taxa.

Fig. 3. Fabrics resulting from intrinsic biofactors. (A) Photomicrograph showing cohesive sand layers (arrows) at the lower and upper part, caused by microbial biomass coating sand grains and filling pore spaces of siliciclastic sediments. Upper part: lamina-specific distribution of heavy mineral grains. Mellum Island, littoral position II (Fig. 2). Scale: 1 mm. (B) Photomicrograph showing an approximately 4-mm-thick layer of condensed fibrillar meshwork that overlies the siliciclastic substrate (lower part, light). Low amounts of sand- and silt-sized quartz grains are incorporated in the organic layer. Mellum Island, littoral position III (Fig. 2). Scale: 3 mm. (C) Section cut from microbial mats growing in Tunisian lower supratidal shallows (littoral position III, Fig. 2). Various filament tufts standing about 1 mm above the basic mat are visible against the light. The vertical section also shows the regular multilayered build-up of biovarvites. (D) Macroscopic surface view of Tunisian microbial mats showing reticulate features produced by tufts, pinnacles and bulges. Features resemble 'elephant skin'. Scale: 10 cm. (E) Surface ornamentation of Tunisian microbial mats: pinnacles and bulges. Pinnacles result from induced polarity changes of filamentous cyanobacteria that also form the basic mats. Bulges are produced by *Lyngbya aestuarii*. Bulges radially merging with pinnacles produce reticulate patterns (upper right corner). (F) Close-up of reticulate patterns on Tunisian mat surfaces produced by dominance of *Lyngbya aestuarii*. Scale: 1 cm. (G) Regular multilayered build-up of biovarvites (dark spots indicate carbonate grains formed biogenically *in situ*). Example from the Solar Lake, Gulf of Aqaba, Egypt (modified after Gerdes & Krumbein, 1987). Scale: 1 cm.

water to much of the sabkha surfaces and shallow depressions. Groundwater prevails some millimetres to centimetres above the surface (III). These are the growth sites of formidable microbial mats dominated by ensheathed filamentous cyanobacteria (*Microcoleus–Lyngbya* mats; Table 1). The areas covered by compact mats appear dark against the reddish mineral bottom of the higher sabkha, which is inundated only sporadically during groundwater high stands or rainfall. Here, evaporite-encrusted microbial films occur, dominated by *Entophysalis* and Pleurocapsalean species (littoral position IV).

MATERIALS AND METHODS

Sedimentary surface structures of Mellum Island and the Tunisian coast were characterized by photography, drawing of serial sections and microscopic studies (Noffke, 1997). Samples of microorganisms were examined by light microscopy. Genera of cyanobacteria were determined according to morphological attributes (Geitler, 1932; Rippka *et al.*, 1979). The determination of species additionally refers to extensive taxonomical studies on cyanobacteria of Mellum Island (Stal & Krumbein, 1985), and of hypersaline microbial mats (Riege, 1991). Undisturbed sediments were obtained with tube corers (15 and 30 cm long, 5 cm in diameter) and Reineck box corers (Reineck, 1970). Slices of the core materials were hardened for thin sections using the Spurr method (Wachendörfer, 1991). Thin sections were studied by light microscopy, and internal structures and components were visualized by image processing. Detailed descriptions of investigation methods used are given by Noffke (1997).

RESULTS

Catalogue of microbial signatures

The catalogue of microbial structural signatures (Table 2) summarizes a collection of sedimentary structures obtained from both study sites. Although the textural geometries reveal a high structural diversity, their characteristics are primarily based on a few major parameters: (1) intrinsic biofactors; (2) biological response to physical disturbances of the growth base; (3) trapping/binding effects; (4) secondary physical deformation of biogenic build-ups; (5) postburial processes; and (6) bioturbation and grazing.

Intrinsic biofactors

Intrinsic biofactors controlling biogenic sedimentary structures are inherent in the organisms, i.e. their construction morphology, growth, taxis and behaviour. In both study sites, the most prominent mat producers are cyanobacteria. Although they are prokaryotes, cyanobacteria are larger and have more defined morphologies than other prokaryotic groups. Their relevance in stromatolite diversification is well known (e.g. Krumbein, 1983).

Species important in this investigation

Morphotypes of benthic cyanobacteria involved in mat and biofilm formation include ensheathed and 'naked' filamentous forms, encapsulated and 'naked' coccoidal forms, cells of random and regular dispersal and colonial aggregation.

The filamentous taxa grow predominantly prostrate, but are also able to erect trichomes in a vertical direction. Most prominent are: (1) ensheathed filamentous cyanobacteria containing either bundled trichomes (*Microcoleus chthonoplastes*) or a single trichome (*Lyngbya aestuarii*); and (2) sheathless filamentous cyanobacteria (*Oscillatoria limosa*).

Microcoleus chthonoplastes forms laminae of condensed fibrillar meshworks (Fig. 3B). Lamina formation can be seen in functional analogy to the weaver's technique of lamina stretching until all filaments are prone. Multiple ensheathed filament bundles are typical of this species. The organisms are able to glide up and down in order to position themselves as close as possible to optimal light intensities. If the surface cover becomes too thick, or light conditions change because of increasing water cover after intermittent exposure, smaller motile cell aggregates, termed hormogonia, are able to respond phototactically and move upwards. They accumulate on the new surface and produce sheath-enclosed filament bundles. The repeated repositioning of horizontally stretched ensheathed filament bundles produces vertical build-ups of condensed fibrillar meshworks (Fig. 4B: structural polarity). *Microcoleus* trichomes can also reorient into a vertical growth position, forming tufts and pinnacles (ministromatolites) that rise some millimetres above the mat surface (Fig. 4B: induced polarity).

Lyngbya aestuarii occurs together with *Microcoleus* mats in Tunisian supratidal shallows and forms characteristic bulges and pinnacles that rise some millimetres above the mat surfaces

Table 2. Catalogue of microbial signatures in peritidal siliciclastic sediments.

Controls on microbial signatures	Textural fabrics Biomass 'cryptic'	Textural fabrics Biomass overgrowing the mineral substrate
A. Intrinsic biofactors		
Morphotypes, growth, taxis	Cohesive sand layers	Condensed fibrillar meshworks Thrombolitic fabrics Tufts, pinnacles Bulges, reticulate networks on bedding planes
Over-riding		Biovarvites
B. Biological response to physical disturbances		
Sediment supply	Biolamination	Biolamination
Erosion	Sinoidal structures Frozen ripple marks	Ripple levelling
Desiccation, cracking		Crack tapestry Bulges protruding above the polygonal cracks
C. Trapping and binding	Lamina-specific selection for heavy mineral grains	Grain orientation according to gravity Laminae lenticular to wavy Sucrosic carbonate crystals coating filaments
D. Mechanical stress acting upon biostabilized surfaces		
Erosion	Erosional pockets Microbial mat chips	Erosional remnants Microbial mat chips
Gas pressure	Soft-ground and evaporite-encrusted domes and folds (petees)	Soft-ground and evaporite-encrusted domes and folds (petees)
Crystallization pressure	Cauliflower-like gypsum rosettes	
E. Post-burial processes		
Organic matter decomposition and gas development		Sponge pore fabrics
Active microbial response to mineral formation *in situ*		Coatings of precipitates by biofilms Concentric laminations around precipitates
Biogeochemical mineral precipitation		Lamina-specific, clustered and dispersed pyrite Lamina-specific, clustered and dispersed carbonates 'Eye structures' 'Frozen filaments'
F. Bioturbation and grazing		
Bioturbation	'Frieze architecture' (sharply projecting bedding surfaces combined with *Skolithos*-like burrows)	Traces of burrowing insects
Grazing	Gastropod shells and faecal pellets containing remains of microbial films/mats	

(Fig. 3F). Evidence of light-dependent movement of this species has been obtained from various studies (e.g. Javor & Castenholz, 1984).

Oscillatoria limosa belongs to the type of 'naked glider' (Golubic & Knoll, 1993). It is a 10-μm-thick, highly motile filamentous species that constitutes a pioneer organism in the intertidal sediments of Mellum Island. Freshly colonized sediment is commonly dominated by this species. In contrast to *Microcoleus* mats, sediments colonized by *O. limosa* contain relatively little biomass. The organisms adhere predominantly to sand grains and fill pore spaces of surface sediments. Such conditions support cohesiveness
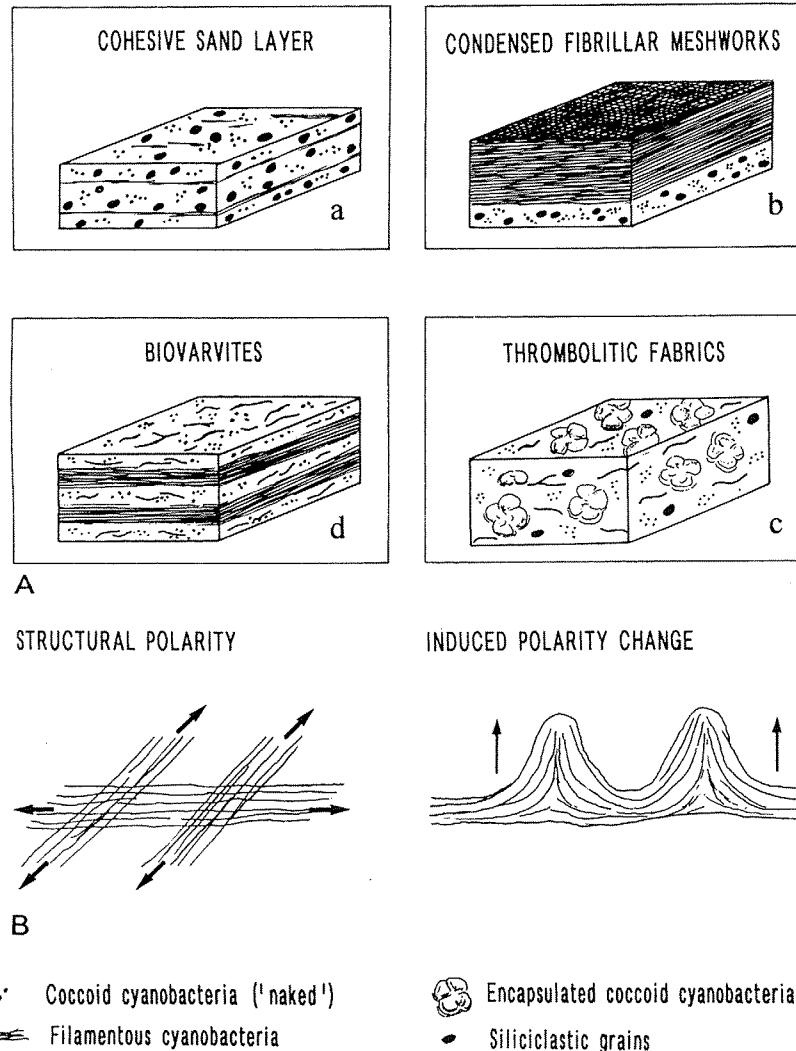
Fig. 4. (A) Basic biofacies types described in this study (see Table 1): (a) cohesive sand layers (cryptic distribution, high clastic mineral contents); (b) condensed fibrillar meshworks protruding above the inorganic substrate have low clastic mineral contents; (c) thrombolitic fabrics caused by coccoidal cyanobacteria dominance; (d) biovarvites representing vertical stacks of couplets of condensed fibrillar meshworks and thrombolitic fabrics. (B) The fibrillar meshwork occurs in two varieties: structural polarity of filament bundles (left); and induced polarity change of filament bundles (right) results in erect tufts and micropinnacles.

of the surface layers without the typical biostromate pattern of biomass overgrowing the siliciclastic substrate (Fig. 3A).

Coccoidal taxa occur predominantly in dispersed or colonial cell arrangements, usually embedded in extracellular polymeric envelopes of variable thickness. Most prominent are: (i) sheathless colonial cyanobacteria that adhere to sand grains (*Merismopedia punctata*); (ii) completely separated cells of 2–3 μm in diameter producing large amounts of slime (*Aphanothece* spp.); and (iii) colonial bacteria that form granular and mammillate structures (*Entophysalis granulosa*, species of the Pleurocapsalean group; Fig. 4: thrombolitic fabrics).

Merismopedia punctata forms characteristic colonies of rectangular, regularly arranged plates of up to 32 cells. It is involved in the formation of cohesive sand layers. Locally, the species is

dominant on Mellum Island intertidal flats (Stal & Krumbein, 1985).

Aphanothece species are responsible for hydroplastic, cushion-like accumulations of extracellular polymeric substances (EPS), in which numerous coccoidal cells of about 4 μm cell diameter are enclosed. Internal fabrics are usually unlaminated or at least poorly laminated. Surfaces reveal smooth patterns. On Tunisian lagoonal margins, the species is the most prominent producer of hydroplastic build-ups that fill each topographic low of the inorganic substrate. Because it stays wet, the mats composed of, or interspersed with, extracellular polymeric substances (EPS) are sluggish to disperse. These several-centimetres-thick hydroplastic pillows appear pink to orange in colour because of the pigmentation of numerous cells that reveal a cluster-like distribution within the EPS.

Entophysalis granulosa and species of the Pleurocapsalean group form cell clusters of granular or nodular appearance. In various hypersaline habitats, internal and surface sediments are commonly disrupted by cauliflower-like structures of up to several centimetres in diameter, made of Pleurocapsalean colonies.

Several mat inhabitants of different morphotypes over-ride each other to gain optimal positions within environmental gradients. Phototactic gliding motility is triggered by changes in light intensities. In the various hypersaline settings studied, phototactic response allows the light-sensitive *Microcoleus chthonoplastes* to avoid the surface in summer. During this period, filamentous mats occur below the surface. On account of EPS production and photoprotective pigments, several coccoid species of cyanobacteria are able to withstand high insolation and evaporative conditions at the surface. *Aphanothece* spp., other coccoids and diatoms thus represent surface populations in summer. In winter, *Microcoleus chthonoplastes* benefits from a lower light intensity and a water level above the sediment, and again overgrows the coccoid surface populations. Such competitive behaviour reveals couplets of light-sensitive winter laminae and hydroplastic summer layers (Figs 3G and 4: biovarvites). Winter laminae usually consist of condensed fibrillar meshworks about 50–100 μm thick, whereas the summer layers can attain a thickness of several hundreds of micrometres, owing to the production of considerable quantities of extracellular slime.

Architectural characteristics

Cohesive sand layers. Local dominance of *Oscillatoria limosa* and/or *Merismopedia punctata* and their preferred adherence to sand grains determines the biolaminite type of cohesive sand layers (Fig. 3A). Characteristic organic layers are about 1 mm thick or less and contain relatively high contents of mineral grains. Binding together of sediments by the microbial biomass and extracellular polymers results in biostabilized surface layers that resist erosion (Führböter & Manzenrieder, 1987). Such layers usually display cryptic positions and never protrude through the siliciclastic substrate.

Condensed fibrillar meshworks. Local dominance of *Microcoleus chthonoplastes* and the predominantly prostrate growth of this species produce a biolaminite that is composed of a complex texture of condensed fibrillar mesh-

works, which significantly overgrow the inorganic substrate (microbial biostrome type; see Glossary). These build-ups can reach several centimetres in thickness. An additional characteristic of this laminite type is the low content of mineral grains (Fig. 3B).

Thrombolitic fabrics. These are unlaminated to poorly laminated, loaf- to mound-shaped structures with a macroscopic clotted fabric. This relates to the local dominance of coccoidal forms enveloped in extracellular polymers, producing separate cells characteristic of *Aphanothece* spp., or nodular cell colonies characteristic of *Entophysalis granulosa* and Pleurocapsalean species (Fig. 4: thrombolitic facies).

Tufts and pinnacles (ministromatolites). Tufts are bundled filaments of *Microcoleus chthonoplastes* and *Lyngbya aestuarii* that originally contribute to the basic mat. Induced polarity changes (see Glossary) cause the filament bundles to reorient into a vertical position and rise some millimetres above the mat base (Fig. 3C). Coccoidal cyanobacteria and diatoms often succeed the filaments and colonize the tufts, producing amounts of EPS that flow around and stabilize the originally soft and flexible tufts. Because of these processes, rigid pinnacles form (Fig. 3C). Water-covered mats commonly have stipes with numerous pinnacles 2–3 mm high and a base 2–5 mm in diameter. In vertical section, pinnacles and tufts contribute to the characteristic wavy appearance of biolaminations.

Bulges and reticulate ornaments on the mat surface. *Lyngbya aestuarii* also forms elongated bulges above the mat. Both bulges and pinnacles form a characteristic relief in which pinnacles represent the focus of radially arranged bulges. Intersecting bulges and pinnacles form a reticulate pattern (Fig. 3D–F) that macroscopically resembles 'elephant skin' (Gehling, 1991). Striking similarities also exist between the reticulate patterns in this study and wrinkle structures described by Hagadorn & Bottjer (1997). When comparing wrinkle structures in Vendian–Cambrian strata with surface structures on modern microbial mats on the coast of Texas, the authors found ample comparative evidence to suggest that the ancient wrinkle structures were likely to have been formed by microbial activity.

Biovarvites. Biovarvites are alternating couplets of laminae produced by two different cyanobacterial morphotypes: (i) ensheathed filamentous cyanobacteria that form condensed laminae of fibrillar meshwork; and (ii) coccoid cyanobacteria excreting EPS, in which the laminae are swollen

by the viscous slime. Along the Tunisian coast, biovarvites form without the aid of sedimentation. Hydroplastic EPS layers appear light against the dark *Microcoleus–Lyngbya* mats (Fig. 3C and G). Biovarvites are formed by the cyclic competitive over-riding process described above (detailed descriptions in Gerdes *et al.*, 1991).

Biological response to physical disturbances

Physical processes that give rise to growth responses of biofilms and microbial mats include: (1) sedimentation; (2) erosion; and (3) fracturing of surface layers as a result of desiccation.

Sedimentation causes burial of the living surface populations. If the sedimentation rate is low, the organisms can evade burial by upward migration to the new surface. Microbial sheaths and slimes are left behind and mark the former mat-covered surfaces (Fig. 3A and B). Sediment blanketing serves as a trigger that forces the buried mobile organisms and trichomes to move upwards and to over-ride the new top layer. Via growth, new surface mats establish themselves. Repetition of these processes results in stacks of biolaminated sand.

Biolaminations represent alternating couplets of sediment and microbial biomass resulting from the interplay between physical processes and biological response. The development of such couplets can be illustrated by the following short-term cycle: (i) in response to burial by sedimentation, the organisms move upwards from buried mats; (ii) as a second biological response to zero sedimentation, the organisms produce new biomass layers; and (iii) during the next burial event, dead biomass is left behind as an organic-rich lamina.

Sediment erosion. Ripple marks are present on Mellum Island tidal flats up to the supratidal zone. Sand blankets on top of mats commonly become rippled before microbial recolonization. The mats then recolonize the rippled surface. The organisms, responding ecologically to the surface undulation, commonly colonize ripple troughs and lee faces. If the surface again becomes activated by an increase in hydrodynamic energy, the less stabile windward faces of the ripple marks may be eroded, and the lee faces with their organic coatings are buried. Sedimentary structures resulting from such coinciding processes are sinoidal organic layers (Fig. 5A; Noffke *et al.*, 1997b).

In the presence of *Microcoleus chthonoplastes*, the production and condensation of biomass on top of the rippled surface can be such that the undulating ripple morphologies become completely filled and levelled (Fig. 5B; Noffke & Krumbein, 1999).

The development of sinoidal structures and ripple levelling can be illustrated by the following short-term sequence: (i) primary physical processes are sedimentation, burial of mats and ripple formation; (ii) as a second process, the biological community responds to burial by upward migration; (iii) during low or zero sedimentation, biomass accumulates. For ecological reasons, the organisms grow and reproduce preferentially within ripple troughs and on ripple lee faces.

On some areas of the tidal flats, ripple marks occur that are fixed by *Oscillatoria limosa* and *Merismopedia punctata*. Biological fixing of the physically generated morphology produces 'frozen' ripples. The ripples form in relation to tidal flushing, whereas the organisms recolonize the surface preferentially after the water drains. The next tide may then reinitiate sediment transport; however, surface patches successfully stabilized by the cohesive matrix may withstand the shear stress. This generates a puzzle of multidirectional 'frozen' ripple marks (Fig. 5C; Noffke *et al.*, 1996; Noffke, 1998).

Significance of fractures in surface layers. Along the Tunisian coast, microbial mats are commonly fractured as a result of desiccation and other stresses, such as gas generation and crystallization pressure. Shrinkage of microbial mats is marked by polygonally arranged cracks (Fig. 5D). The edges of cracks are usually rounded, because fracturing enables the mat-forming microbes to overgrow the margins and evade the cracks. Overgrowth of margins results in pillow-like structures, bulges and pocket-like, multilayered crack tapestries (Fig. 5E and F). Former cracks are also indicated by bulges of organic matter that protrude above the mat surface in a polygonal pattern (Fig. 5E).

Trapping/binding processes

Trapping is the process by which sediment particles are glued to the sticky mat surface. The term binding means that the deposited or trapped allochthonous material becomes enclosed within the growing mats or biofilms. Binding is sometimes triggered by 'baffling', a process by which filamentous cyanobacteria stretch upwards forming an organic 'comb' perpendicular to the mat surface. The trichome bundles standing upright
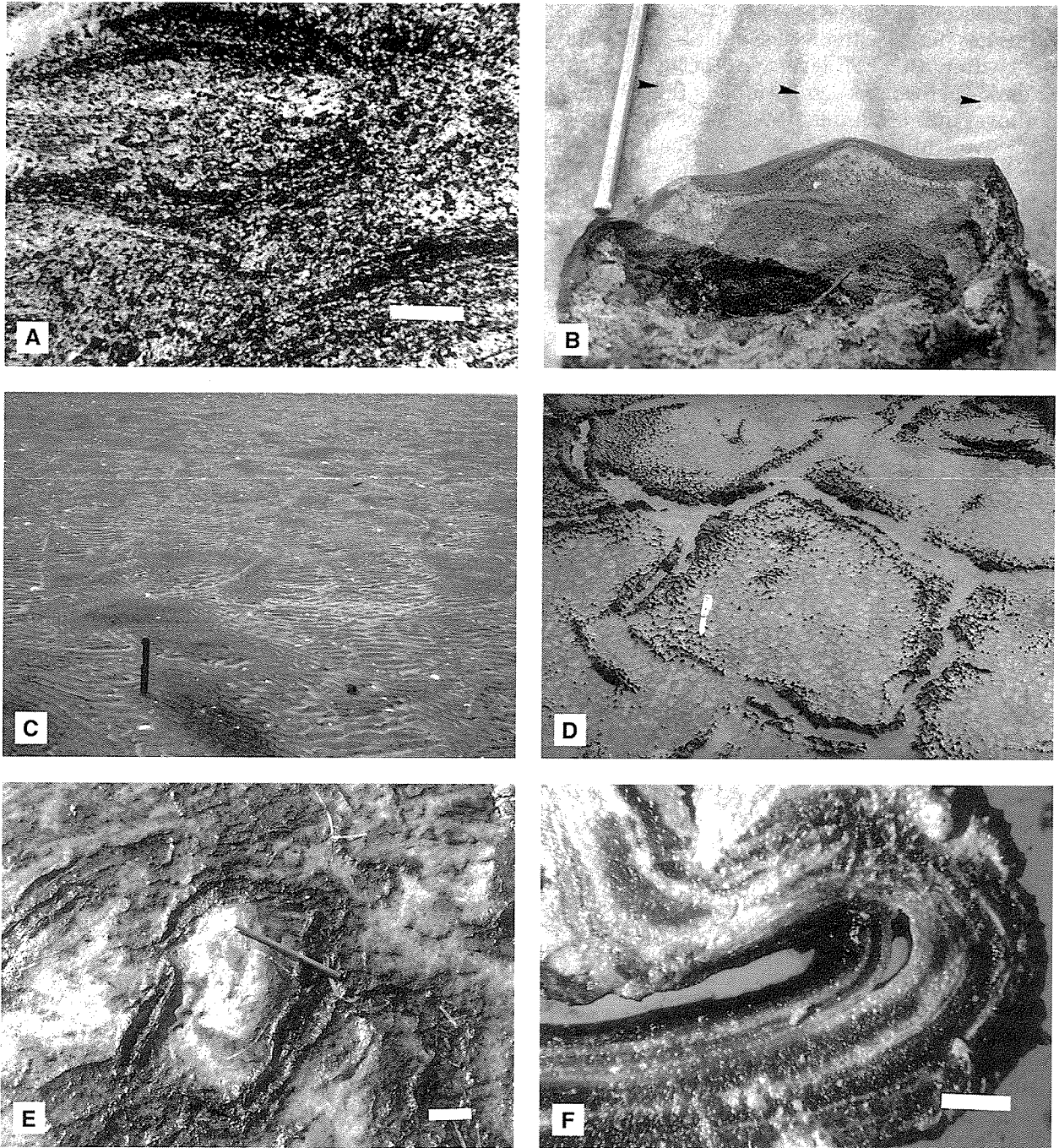
Fig. 5. Fabrics resulting from biological response to physical disturbances. (A) Photomicrograph showing sinoidal structures (dark) resulting from microbial biomass that drapes ripple marks. Mellum Island, littoral position II to III (Fig. 2). Scale: 1 cm. (B) Photograph of biogenic ripple levelling. Surface view (upper light part) and cross-section (lower part). Surface view: ripple marks show through the microbial mat (arrow). Vertical section: several generations of ripples are visible with ridges draped and ripple troughs filled by condensed biomass produced by microbial mats (after Noffke & Krumbein, 1999). (C) Multidirectional ripple marks on tidal flats of Mellum Island that were generated from the repeated change between physical sedimentation and transport on the one hand and microbial colonization and fixation of ripple marks on the other hand (see text; after Noffke, 1998). (D) Polygonally cracked microbial mats covered by a thin salt coating. Internal flats are ornamented by pinnacles that project through the salt cover. Reticulate pattern of surface mats shows through the salt cover. Edges of polygons are draped by bulges and upfoldings (dark) of the basic mat. The white knife is 12 cm. (E) Re-establishment of microbial mats within cracks of the basic mat. The pencil is 16 cm. (F) Pocket-like multilayered crack tapestry produced by microbial mats that grew into the cracks of surface mats (compare with E). Scale: 1 cm (D–F: Tunisian microbial mats).

create microzones of lower current velocity that aid the settlement of smaller grains.

In this study, trapping and binding processes give rise to: (1) oriented grains and wavy to lenticular laminae; (2) lamina-specific grain arrangements; and (3) 'sucrose' calcium carbonate accumulations.

Grain orientation and wavy to lenticular laminae. In biolaminites composed of condensed fibrillar meshworks, enclosed quartz grains are commonly matrix supported and arranged with their long axis parallel to the sedimentary surface (Fig. 6A). Such orientation may result from the incorporation of grains by trapping/binding and

reduction of mechanical friction by the soft matrix surrounding the quartz grains, which aids the rotation of the grains to an energetically suitable position. In grain-supported interlayers between mat horizons, grains are not oriented with their long axes parallel to the sedimentary surface. This may indicate that, in closely packed sediments, a gravity-related orientation is not possible (Noffke *et al.*, 1997a).

A signature of trapping/binding also common in the condensed fibrillar meshworks is the arrangement of lenticular to wavy laminae surrounding individual quartz grains. These structures are produced by microbial sediment binding
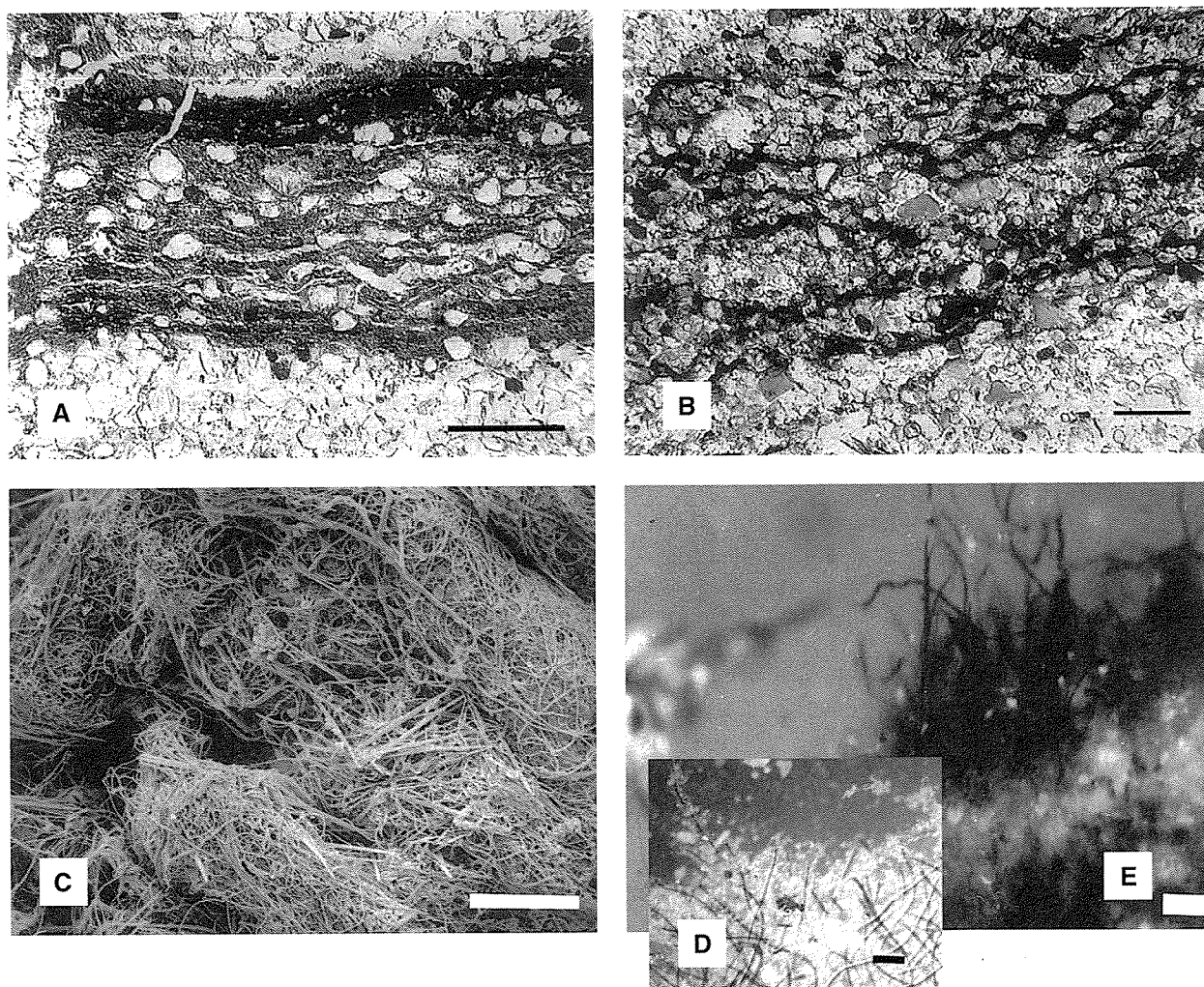
Fig. 6. Fabrics resulting from trapping and binding. (A) Matrix-supported quartz grains incorporated in the fibrillar meshwork of a *Microcoleus* mat, arranged with their long axes parallel to the sediment surface. Scale: 1 mm. (B) Photomicrograph showing wavy to lenticular laminae enclosing individual quartz grains (compare with C). Scale: 1 mm. (C) Fibrillar meshwork of filamentous cyanobacteria completely masks sand grains, perceptible by rounded shapes (Mellum Island). Scale: 200 μm. (D) Sugary microcrystals of calcium carbonate sprinkling microbial filaments that stretch upwards perpendicular to the mat surface. (E) White amorphous carbonate cluster below the erect filaments may have been incorporated into the mat material as a result of 'binding' (see Glossary). (D and E: Tunisian microbial mats; scale: 1 mm).

as a biological response to the sediment supply to the mat surface (Fig. 6B and C).

Lamina-specific grain selection. A specific feature of biolaminated quartz sands is the lamina-specific selection for heavy mineral grains (Fig. 3A). Although still unclear, the genesis of these features may be related to trapping/binding processes mediated by the sticky and slowly vertically accreting surface mats.

'Sucrose' calcium carbonate accumulations. Under water, cyanobacteria of the *Microcoleus–Lyngbya* mats were observed to stretch filaments upwards perpendicular to the mat surface. The filaments often have a sprinkling of sugary microcrystals of calcium carbonate (Fig. 6D). Their origin may be closely related to the establishment of a microzone of slightly increased salt concentration close to the mat surface, triggered by the organic comb of trichome bundles that provide calm microenvironments. Owing to the binding activities of the microbial communities, such 'sucrose' calcium carbonate accumulations at the mat–water interface may give rise to features that resemble micrite clusters (Fig. 6E).

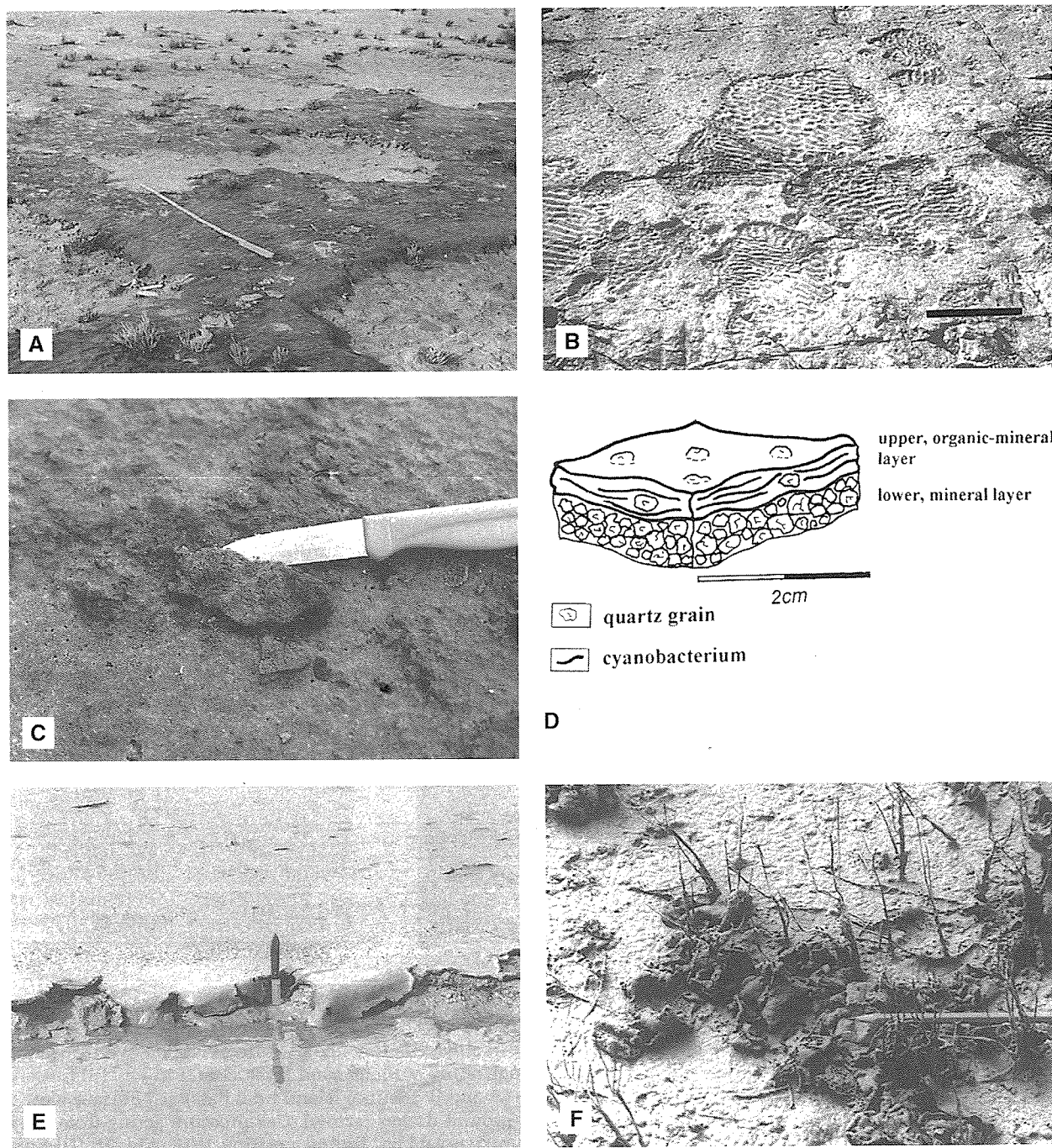### Mechanical deformation of biostabilized sediments

Mechanical stress acting upon sediments overgrown and biostabilized by biofilms and mats before the stress give rise to: (1) erosional structures; and (2) overthrust structures.

Erosional fabrics. The surface morphology of the sampling sites of Mellum Island is characterized by two main erosional signatures of biostabilized sediments (Fig. 7A): erosional remnants, i.e. sharply projecting planar rises covered by microbial mats and protruding up to several centimetres above the surrounding sediment; and erosional pockets, i.e. rounded depressions of about 10–50 cm diameter, with sharp to gradual margins. Both signatures indicate erosional stress acting upon the biostabilized sediments (see detailed descriptions of erosional remnants by Noffke & Krumbein, 1999; erosion pockets by Reineck, 1979). The distribution of both erosion structures suggests different degrees of biostabilization resulting from the interaction of currents and waves and the composition and stage of maturity of the stabilizing microbial communities. The dominant supratidal form *Microcoleus chthonoplastes* is able to overgrow the inorganic substrate completely and stabilizes the sediments more successfully than the dominant intertidal form *Oscillatoria limosa*. An analogous fossilized

bedding plane is well displayed in the Cretaceous Dakota Group at Alameda Avenue (Fig. 7B; MacKenzie, 1968).

Similar patterns evolve according to the formation and distribution of mat chips, i.e. organosedimentary fragments of biostabilized sedimentary surfaces (Fig. 7C and D). If hydrodynamic forces increase, the biologically stabilized sediments are eroded from their source area. However, the individual mineral grains are not completely separated. Small chip-like relics, i.e. organically bound mineral aggregates of the formerly preconsolidated surface, remain. These relics are termed 'microbial mat chips'. In the study areas, erosional stress, scour and wash marks, even gas formation related to microbial primary production and decomposition, are mainly involved in their formation. Types of mat chips are distinguished according to their form, load of quartz sand, transportation and deposition behaviour. These types can be traced back to distinct source regions in the littoral area. Type 1 derives from microbial mats forming cohesive sand layers (Mellum Island), or dominated by coccoidal cyanobacteria (Tunisian coastal areas; Fig. 7E and F). Type 2 derives from microbial mats forming condensed fibrillar meshworks caused by *Microcoleus chthonoplastes* (Fig. 7C and D). Type 2 mainly occurs on Mellum Island, where erosion is acting upon mats up to the lower supratidal range (see erosional remnants, Fig. 7A).

Overthrusting as a result of gas pressure. A specific kind of mechanical stress acting upon the biosedimentary matrices is maintained by the production and diffusion of gas in the internal sediment bodies. This factor is operating at both areas of deposition. Principally, the stress acts against the mat-secured sedimentary surface from below, as diffusion of the intrasedimentary gas is primarily directed upwards. Both Mellum Island and Tunisian coastal sabkhas reveal a variety of surface deformation caused by gas formation in the substrate (Fig. 8A–D). Results are domes and folds with a hollow centre and generally a circular or elongated base. On Mellum Island, the hollow spaces are filled with methane. The gas migrates from deeper buried organic deposits, through internal gas channels towards the surface. Here, the cohesive microbial tissues inhibit escape of the gas into air or water. When accumulating beneath the surficial mat, gas pressure leads to doming of the mat (soft-ground domes; Fig. 8A and B). In arid settings, soft-substrate domes are immediately encrusted by gypsum (Fig. 8C). After rewetting, such domes are
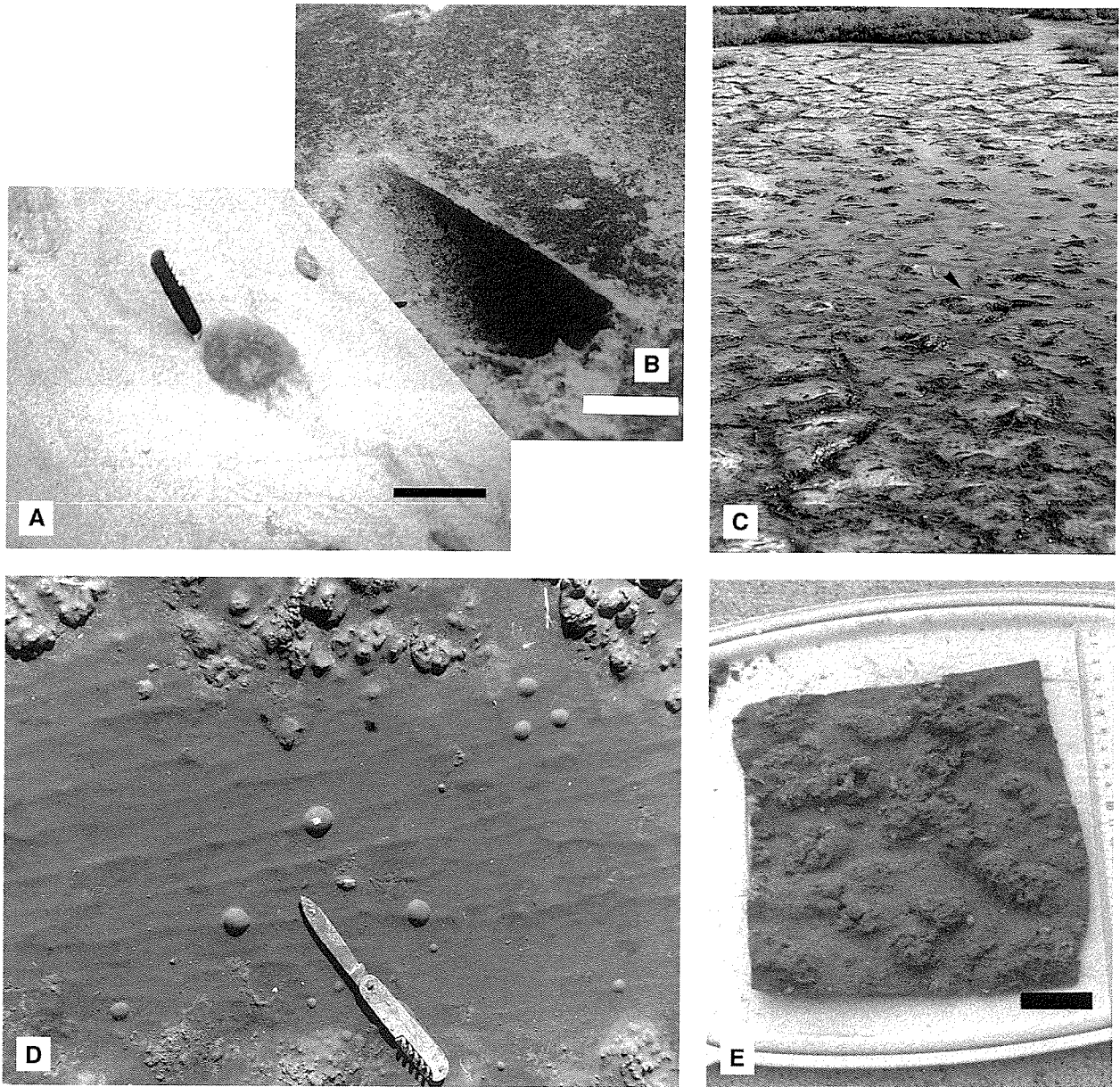
Fig. 7. Fabrics resulting from mechanical deformation of biostabilized sediments. (A) Erosional fabrics of biostabilized sedimentary surfaces on Mellum Island: sharply projecting planar rises (erosional remnants) and rounded depressions (erosion pockets) of about 10–50 cm diameter (modified after Noffke, 1999). (B) An analogous fossilized bedding plane is well displayed in the Cretaceous Dakota Group at Alameda Avenue (modified after MacKenzie, 1968). Scale: 20 cm. (C) Microbial mat chips of irregular shape and size on the tidal flats of Mellum Island. (D) Schematic view of a mat chip with associated inorganic substrate. (E) microbial mats hanging over the edge of the lagoon at Bahar Alouane, Tunisia, giving rise to the genesis of mat chips. (F) Mat chips accumulated around dead salt marsh plants (Tunisia).

commonly overgrown by microbial mats ('petees'; detailed descriptions and discussions are given by Reineck *et al.*, 1990).

Overthrusting as a result of crystallization pressure. The surface sediments of Tunisian coastal sabkhas are stabilized by a mixture of

Fig. 8. Fabrics resulting from mechanical deformation of biostabilized sediments. (A) Microbial mat overthrusted by methane formation in the internal sediment body; arch through a thin surficial sand layer. Scale: 15 cm. (B) Close-up of dome opened to show internal hollow space. Scale: 3 cm. (A and B: Mellum Island tidal flats). (C) Surface view on microbial mats resembling a tiled floor, resulting from soft ground domes (arrow). Gas pressure acting from below causes cracking around the circular base of the domes (Tunisian sabkha, littoral position II/III, Fig. 2). (D) Small gypsum-encrusted domes and folds cover the sedimentary surface of a Tunisian sabkha (littoral position IV, Fig. 2). Upper part: cauliflower-like gypsum rosettes. (E) Section cut from microbial mats covered by cauliflower-like gypsum rosettes. Structures are made by dominance of coccoidal cyanobacteria. Scale: 3 cm.

coccoidal microbes, clay and gypsum crystals. Numerous cauliflower-like gypsum rosettes, with a basal diameter of about 2 cm and 1–2 cm high, protrude above the smooth surface (Fig. 8D and E). These structures, which resemble small biscuits, are characteristic of *Entophysalis granulosa* and Pleurocapsalean species. However, their enlargements and common cracks suggest the additional influence of lateral crystallization pressure.

Post-burial processes

This section summarizes: (1) textural fabrics evolving from mechanical effects of gas formation from decaying microbial mats; and (2) features

related to the formation of authigenic minerals (calcium carbonate and pyrite). Mineral precipitation, in general, is facilitated in microbial mats because of the enrichment of biomass by microbial primary producers, followed by its decomposition and the biogeochemical cycling of matter and energy within the sediments.

'Sponge pore sand' and diffusion of biogenic gases

Commonly, lamina-concordant cavities several millimetres in diameter are intercalated in siliciclastic interlayers between the organic laminae representing former microbial mats. The cavities are arranged like pearl strings and indicate that gas diffusion has taken place in the biolaminated sequence. Analyses revealed the presence of CH_4, CO_2 and H_2S (Noffke *et al.*, 1996). The geometry of pore arrangement resembles the constructional morphology of sponge skeletons, so the term 'sponge pore sand' has been proposed (Noffke *et al.*, 1996). The regular distribution of pores resembling sponge fabrics is maintained by the buried mats. Organic matter, consisting of empty abandoned sheaths, immotile organisms and various amounts of EPS, provides cohesive strength, which results in a significant delay in upward gas migration. Viscous EPS is able to lower the diffusion velocity by at least a factor of 10 (Krumbein, 1983). Participating processes in the development of these specific sedimentary structures are: (1) the production of biogenic gases resulting from the decomposition of organic matter; (2) gas diffusion; (3) decrease in diffusion velocity of reactive gases caused by the intercalated cohesive organic layers; and (4) mechanical pressure of the gas entrapped in the siliciclastic interlayers. Gas pressure greater than the resistance of the sand grains finally results in the formation of fenestrae-like cavities (Fig. 9A and B).

Microbial coating of interfaces

Coatings. The internal mat provides a variety of substrates on which microbes attach, forming the next bacterial film, including clasts, shells, evaporite crystals, pellets and autochthonous minerals. Scanning electron microscope (SEM) studies revealed that almost all solids in the mats are coated. Even the rigid capsular and sheath material produced by coccoid and filamentous cyanobacteria and gas bubbles derived from metabolic products (e.g. O_2, CO_2, NH_3, CH_4, H_2S) provide interfaces for biofilm development.

Concentric laminations. Similar to hypersaline microbial mats from various other semi-arid settings, such as Gavish Sabkha (Gulf of Aqaba, Egypt) and Lanzarote salt works (Gerdes & Krumbein, 1987; Gerdes *et al.*, 1993), the biolaminated deposits along the Tunisian coast harbour a wealth of non-skeletal carbonate particles, including ooids and oncoids. Ooids are spherical to oval particles, in which one or more laminae concentrically coat a common nucleus (Fig. 9C and D). Colours of laminae alternate between dark and light; dark laminae usually being thinner (ranging from 1 to 3 μm in thickness) than the light laminae (5–20 μm). The mineralogy of the light laminae is microcrystalline to cryptocrystalline aragonite. The dark laminae are dominated by organic matter. SEM analyses of the dark laminae show bacterial filaments, EPS and cell clusters of coccoids. The oncoids are particles with partially overlapping laminae around a nucleus. These particles are subrounded, spheroidal or elongated. Sizes range from 100 to 500 μm.

Microstructural analyses clearly indicate the construction of concentric lamination by biofilm attachments to nuclei present in the mats, subsequent aragonite encrustation and additional biofilm attachment. As a result of this sequence, coated grains develop that bear the internal structures of ooids and oncoids (detailed descriptions and discussions of microbial mat-generated coated grains are presented in Gerdes *et al.*, 1993).

Experiments with laboratory-cultured bacteria have provided clues to the mechanism of carbonate precipitation controlled by microbial activity (Krumbein, 1974; Riege, 1991; Chafetz & Buczynski, 1992). Most of these studies suggest that complex biogeochemical reactions during bacterial degradation and transformation of organic matter are responsible, including dark CO_2 fixation, anaerobic respiration and fermentation, uptake and transfer of CO_2, ammonia production and variations in alkalinity and pH.

Early diagenetic pyrite

In microbially mediated build-ups, the formation of pyrite is widespread. Aggregates form in relation to the activity of sulphate-reducing bacteria that benefit from the *in situ* production of organic matter and the presence of sulphate dissolved in surface and porewater. Geologically important products from these processes are: (1) hydrogen sulphide; (2) calcium carbonate,
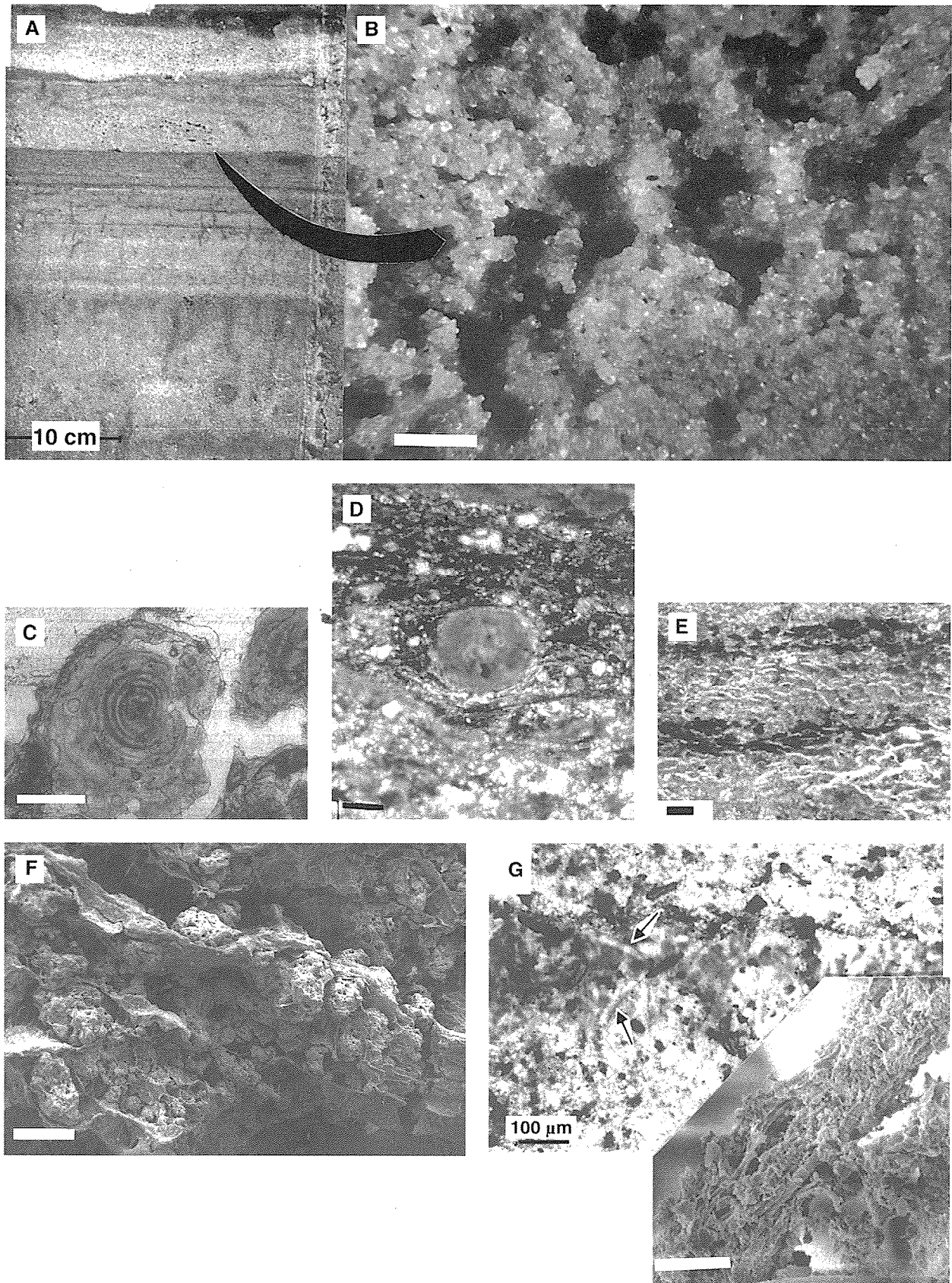
Fig. 9. Fabrics resulting from post-burial processes. (A) Vertical section showing various buried microbial mats. Arrow: sponge pore sand. Fenestrae-like cavities are caused by gas diffusion. Buried microbial mats provide cohesive strength that results in a significant delay during upward migration of the gas (Mellum Island; after Noffke, 1997). (B) Close-up of sponge pore sand visible in (A). Scale: 2 mm. (C) Carbonate particle that has formed in a hypersaline microbial mat showing internal laminations that concentrically coat a nucleus (benthic ooid, Lanzarote salt works; after Gerdes *et al.*, 1993). Scale: 100 μm. (D) Carbonate grain enveloped by microbial filaments (Tunisian mat). Scale: 100 μm. (E) Photomicrograph showing pyrite enrichment in laminae enriched in rigid sheath materials, Tunisian coastal area (after Noffke, 1997). Scale: 100 μm. (F) Lamina-specific arrangement of carbonate grains closely linked to laminar build-ups of biovarvites (Lanzarote saltworks; after Gerdes *et al.*, 1993). Scale: 500 μm. (G) Vertical section through microbial sediments showing various vertically and diagonally oriented cyanobacteria filaments coated by envelopes of calcium carbonate (arrows). Right: photomicrograph showing a coated filament bundle. Scale: 50 μm.

native sulphur and pyrite (Friedman *et al.*, 1992). In the sediments studied in this investigation, characteristic textural fabrics include lamina-specific, clustered and dispersed pyrite accumulations, which indicate the close linkage of pyrite formation to organic compounds, and microstructures that occur in great diversity within the microbial mats. In thin sections, lamina-specific pyrite accumulations trace: (1) interfaces between laminae of different consistency (e.g. boundaries between fibrillar meshworks and thrombolite fabrics, and boundaries between biogenic and siliciclastic laminae); (2) laminae enriched in rigid sheath materials (Fig. 9E); and (3) cell clusters embedded in EPS, capsules and cell envelopes produced by coccoidal cyanobacteria, internal secondary pores and fenestrae and shells of microfossils, such as diatoms, foraminifera and ostracods.

Polysaccharids, proteins and many other substances of microbial mats are readily mineralized by heterotrophic bacteria. More resistant to mineralization is the fibrillar substance that is embedded in or makes up large portions of the sheath material. These less degradable substances, and those only partially decomposed, provide a variety of moulds for mineral coatings, including pyrite and calcium carbonates (see below).

Early diagenetic calcium carbonate

Eye structures. A characteristic structural record imparted by growing particles in the biolaminated fabrics is termed 'eye structures' (Dahanayake & Krumbein, 1986). Particles formed biogeochemically within microbial laminae can compress and even tear apart adjacent filament bundles. In the living mat, decomposition and mineral formation can start a few millimetres below the surface mat. Thus, living organisms of the phototrophic mat community are still in contact with the zone of mineral formation. The formation of eye structures is usually the product of active responses of the microbiota to a disturbance by the growing

particle. The active growth response results in binding of the mineral grains together by the fibrillar matrix that completely envelops such *in situ* formed particles (Fig. 9D).

Lamina-specific and dispersed distribution of carbonate grains. Similar to pyrite, the distribution of carbonate particles occurs in lamina-specific patterns as well as being clustered or dispersed. Lamina-specific arrangements are closely linked to interfaces presented by the laminar build-ups of biovarvites (Fig. 9F). A clustered and dispersed distribution of particles can be observed within the hydroplastic build-ups dominated by *Aphanothece* spp. The particle distribution apparently follows the irregular positions of individual cells and cell clusters embedded in the viscous gel.

'Frozen' filaments, ghosted remains and moulds

Studies reveal filaments preserved in vertical orientation in carbonate precipitates (Fig. 9G). Such 'frozen filaments' may be indications of premortem embedding. Decay starts immediately beneath the surface mat. The process may be seen as analogous to gut bacteria, which start to decay after the death of the host organism (Allison, 1988). Upon death, microbial cells may be destroyed within hours or days. However, early decay is inhibited where concretionary growth of carbonate precipitates occurs. Many filaments and unicells agglutinated in the calcium carbonate concretions may have suffered encrustation in life position and died with progressing mineralization. Thus, the cells embedded in the carbonate matrix record their mortem rather than their post-mortem history.

Bioturbation and grazing

Modern sedimentary environments inhabited by microbial films and mats reveal various traces of fauna. Along the southern North Sea coast,

siliciclastic microbial mats are contoured by dwelling burrows of marine invertebrates, grazing structures of fish (mullets) and oyster catchers (Gerdes & Krumbein, 1987). Shinn (1972) described the unique association between living cyanobacterial build-ups and burrowing worms on intertidal flats in the Persian Gulf.

This section summarizes: (1) the spectacular features of *Skolithos*-type dwellings characteristic of Mellum Island (termed 'frieze architecture'); (2) traces of burrowing insects occurring at both settings studied; and (3) gastropods and faecal pellets that also contribute to the sedimentary record at both sites.

'Frieze architecture'. On Mellum Island, the intertidal sediments harbour a diverse endobenthic fauna. As a result of extensive bioturbation in these areas, primary physical bedding structures rarely exist. With increasing topographic height towards the mean high water line (MHWL), there is a remarkable coincidence between the development of: (1) sharply projecting bedding planes; and (2) a change from mottled bioturbation structures towards *Skolithos*-type dwellings (Fig. 10A). The sharply projecting bedding planes result from microbial communities that, in response to burial, bind and stabilize each new sedimented surface layer. The *Skolithos*-like structures can be traced to an ecological selection by faunal species that are semi-sessile and do not leave their burrows or tubes except in response to burial or erosion. The burrowing and tube-forming animals are surface feeders and require a connection with the surface. The microbes, on the other hand, also need surface contact for photosynthetic requirements. Thus, both groups keep pace in response to burial. Characteristic of the upper intertidal and lower supratidal areas studied is a pulsed sediment supply resulting from spring tides. Both the pulsed sediment supply and the response of the biota result in
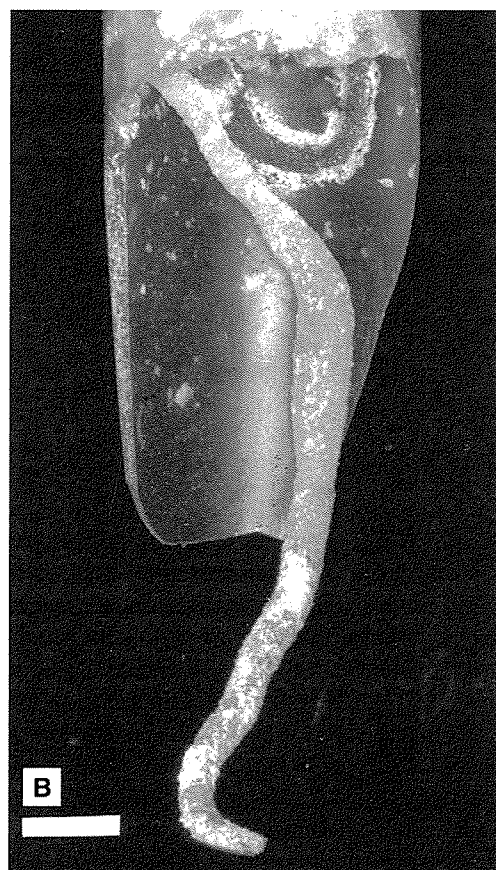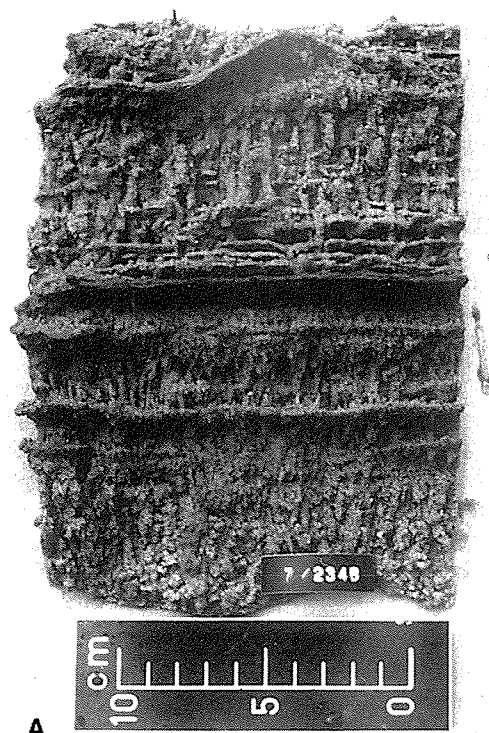
Fig. 10. Fabrics resulting from bioturbation. (A) Relief cast of tidal sediments of Mellum Island. Sharply projecting edges are microbial mats that repeatedly became buried by quartz sand. Vertically oriented structures are dwelling burrows of endobenthic marine amphipods and polychaetes that thrive in the sediments and graze upon the microbial films and mats. (B) Resin cast of the burrow of the salt beetle *Bledius spectabilis* showing the characteristic bottleneck structure. At both study sites, beetles of the genus *Bledius* form these characteristic bottleneck-shaped burrows in microbial build-ups consisting of condensed fibrillar meshwork (Fig. 3B).

conspicuous multistorey structures, termed frieze architecture (Gerdes & Reineck, 1987).

The fauna producing *Skolithos*-like burrows are able to settle above MHWL. However, the local abundance of *Microcoleus chthonoplastes* results in the formation of compact fibrillar meshworks protruding from the siliciclastic substrate (see Fig. 3B). Such conditions exclude almost all burrowing marine species from these areas. There are two reasons for this 'killer mat' phenomenon. First, burrowing animals must expend a great deal of energy to penetrate through such thick filamentous surface layers, and it is not worthwhile for the animals to feed on the mats themselves, because few of them have the specialized mouth parts necessary to rip away at such a tough substrate. The second reason is that the large amounts of biomass cause changes in the sediment. Oxygen becomes limited, and H_2S concentrations increase. These conditions are detrimental to tube and burrow dwellers.

Traces of burrowing insects. A characteristic bioturbation feature of the compact and mainly anoxic biolaminations are burrows built by insects. Both on Mellum Island and in Tunisia's supratidal shallows, as well as in various other microbially colonized hypersaline settings, such as Solar Lake and Gavish Sabkha (Gulf of Aqaba, Egypt), burrowing salt beetles of the staphilinide genus *Bledius* are abundant. These beetles form characteristic bottleneck-shaped burrows within the mats (Fig. 10B; Gerdes & Krumbein, 1987). The compact hypersaline mat along Tunisia's coastal areas also reveals similar traces.

Gastropods and faecal pellets. At both study sites, gastropod shells from nearby living populations are important components of the microbial sediments. In Tunisia's lagoons, abundant cerithid gastropods graze on microbial mats and are able to destroy them completely. The lagoonal margins are commonly covered by layers of numerous gastropod shells. Faecal pellets containing degraded remains of microbial mats contribute to the sedimentary record in this zone. The increasing hypersalinity towards the supratidal zone limits the distribution of the gastropods and excludes them from the most prolific mat-forming environments.

On Mellum Island, both shells and faecal pellets of the small gastropod *Hydrobia ulvae* can be found in the biolaminated deposits. This species, although grazing on cyanobacteria and diatoms, does not destroy the microbial surface films and mats. Grazing is indicated by the accumulation of faecal pellets that contain degraded remains of the microbial species mainly responsible for the formation of cohesive sand layers (see Fig. 3A).

Geographical factors

Comparing the study sites, similar, but also different, distributions of microbial signatures can be found (Table 3).

Intrinsic biofactors

Signatures occurring in both settings are cohesive sand layers and condensed fibrillar meshworks. The topographic shallows of the lower supratidal zone of both settings (littoral position III) support highly productive microbial mats, dominated by the cosmopolitan species *Microcoleus chthonoplastes*. Thick fibrillar meshworks protrude above the inorganic substrate. The adjacent flats of both settings are characterized by cohesive sand layers produced by microbes that adhere predominantly to sand grains.

Signatures only occurring in Tunisian settings are the hydroplastic cushions and thrombolitic fabrics developing from coccoidal cyanobacteria and the tremendous abundance of extracellular polymers they excrete. These also form couplets together with *Microcoleus–Lyngbya* mats in biovarvites. Another characteristic feature of the Tunisian mats is the surface ornamentation that evolves from reticulate bulges and pinnacles. The lack of *Lyngbya aestuarii* on Mellum Island may explain why this ornamentation is lacking there (Table 3).

Biological response to physical disturbance

This kind of interaction produces biolaminations generated by alternating processes of deposition and microbial growth. These typical signatures develop in both settings. While the vertical accretion of microbial biomass reflects periods of no or low sedimentation, the mineral interlayers represent periods of deposition. On Mellum Island, thickness and sediment contents within the biogenic laminae change in accordance with littoral positions. In the intertidal range (positions I and II), laminae are thin and contain relatively large numbers of quartz grains (Fig. 3A). In the supratidal range (sampling position III), longer periods of non-deposition prevail, reflected by the occurrence of condensed fibrillar meshworks containing only small quantities of finer grained quartz (Fig. 3B).

Table 3. Distribution of textual signatures of microbial activity in the two study areas.

	Mellum Island, southern North Sea			Southern Tunisian coast			
	Littoral positions (see Fig. 2)						
	I	II	III	I	II	III	IV
Fabrics due to intrinsic biofactors							
Cohesive sand layers	*	*		*			*
Thrombolitic fabrics					*		
Condensed fibrillar meshworks			*			*	
Tufts, pinnacles						*	
Bulges, reticulate ornamentics						*	
Biovarvites						*	
Fabrics due to biological response to physical disturbances							
Biolamination		*	*			*	*
Sinoidal structures		*	*				
Frozen ripples		*					
Ripple levelling			*				
Polygonal bulges and folds						*	
Fabrics due to trapping/binding							
Grain orientation			*			*	
Laminae wavy to lenticular			*			*	
Lamina-specific heavy mineral grains	*						
'Sucrosic' calcium carbonate						*	
Fabrics due to mechanical deformation of biologically stabilized surfaces							
Microbial mat chips		*	*	*	*	*	
Soft-ground gas domes		*	*	*	*		
Erosional pockets		*					
Erosional remnants			*				
Cauliflower-like gypsum rosettes							*
Fabrics due to post-burial processes							
Sponge pore sand			*			*	
Organic coatings			*		*	*	*
Coated grains					*	*	
Lamina-specific pyrite			*			*	
Pyrite clustered and dispersed			*		*	*	
Lamina-specific carbonate							
Carbonate clustered and dispersed					*	*	
Fabrics due to bioturbation							
'Frieze architecture' (*Skolithos*-type)	*						
Traces of borrowing insects		*				*	*

In Tunisian settings, only thin sand laminae of some hundreds of micrometres thickness are intercalated with microbial mats. At various vertical depths, the sediments additionally contain clay layers a few centimetres thick. The thin sand layers mainly reflect aeolian deposition, after which the microbial populations react by upward migration. The thick clay layers originate from occasional sheet floods. From observations in similar environments subject to sheet floods, it is assumed that, even if the thick clay layers completely seal the microbial populations, organisms held in suspension may inoculate the new sediment surface and initiate new mat generation (Gerdes & Krumbein, 1987).

Signatures only occurring at Mellum Island developed from biological responses to ripple morphologies (sinoidal structures, ripple levelling, frozen ripples). This is because of the strong tidal regime, which is lacking in Tunisia. On the other hand, microbial communities in Tunisia are exposed to climatic effects, such as strong light intensities, high temperatures and evaporation. When responding to this set of physical stresses, the microbial community, which is not significantly different from that of Mellum Island,

produces completely different structures (Fig. 5D and E).

Trapping and binding

A signature occurring in both settings is the orientation of grains in association with the biolaminite type of condensed fibrillar meshworks. A similar occurrence also exists in relation to the wavy to lenticular lamina formation around quartz grains. No grain orientation is visible in the cohesive sand layers that have much thinner organic laminae supported by high quantities of quartz grains.

Lamina-specific enrichments of heavy mineral grains, commonly observed in thin sections from Mellum Island, have never been observed in sediments from Tunisia's coastal areas. On the other hand, the characteristic 'sucrose' calcium carbonate crystals coating filaments of Tunisian surface mats rarely, if ever, occur in microbial mats of Mellum Island.

Mechanical deformation of biologically stabilized sediments

Microbial mat fragments and soft-ground gas domes are produced by the interaction of biogenic matrices with mechanical deformation processes in both settings (Table 3). This may provide a climatic indicator when evaporites encrust the soft-substrate domes in arid settings. Specific to arid settings is the lateral expansion pressure from crystal growth that provides overthrust structures in the form of petees and tepees (Warren, 1982). Expansion pressure from crystal growth is also involved in the formation of the small cauliflower-like, gypsum-encrusted rosettes characteristic of the middle part of the Tunisia sabkhas.

Post-burial processes

Sponge pore sand is found in both settings. This structure evolves from the interplay of both internal gas production and the sealing effects of buried biolaminations. This structure is most abundant where compact buried biolaminites effectively lower the diffusion rates of internal gases. In both settings, the lower supratidal shallows support the development of sponge pore sand. Organic coatings of internal particles are most common in the presence of compact and diverse microbial biolaminites. Tunisian settings commonly favour such coatings on evaporite

crystals. Finally, pyrite arranged in lamina-specific, clustered and dispersed patterns are features in both settings.

On Mellum Island, the formation of authigenic calcium carbonate was observed within the compact organic layers of *Microcoleus* mats (Kropp *et al.*, 1997), and thus occurs in both areas. However, coated grains and other types of carbonate particles, as well as their arrangement in lamina-specific, clustered and dispersed patterns, and 'frozen' filaments embedded in carbonate matrices, are abundant only in Tunisian microbial build-ups.

Bioturbation and grazing

Traces of burrowing beetles, of the same genus that dwell within the compact mats, occur in both settings. Beetle colonies also occur in sediments of the higher lying sabkhas, where cryptic cyanobacterial films still prevail. Shells and faecal pellets of gastropods contribute to sedimentary structures in both settings. However, both gastropod taxa and the degree of mat destruction are not comparable. In Tunisia, highly destructive grazing occurs by cerithid gastropods; on Mellum Island, less destructive grazing is attributable to *Hydrobia ulvae*.

The characteristic 'frieze architecture' composed of sharply projecting bedding planes and *Skolithos*-like dwellings occurs only on Mellum Island. This is caused by the effects of the tidal amplitude that supports the distribution of marine fauna up to the lower supratidal zone.

DISCUSSION

This catalogue comprises a basic set of ubiquitous signatures. The uniformity in architectural characteristics is probably attributed to the presence and local dominance of ubiquitous microbial architects throughout the different settings. One prominent example is the condensed fibrillar meshworks produced by the cosmopolitan *Microcoleus chthonoplastes*. In contrast, the catalogue documents signatures extremely sensitive to: (1) tidal positions; and (2) overall climatic conditions. These kinds of signatures, e.g. biovarvites or frozen ripples, indicate narrow facies zones that often coincide with the activity or dominance zones of certain organisms (Noffke *et al.*, 1996). This strong coupling of sedimentary structural and specific microbiological patterns offers an opportunity to correlate ecophysiological

Table 4. Survey of fossil microbial signatures from siliciclastic, evaporitic or mixed depositional environments.

Author	Structures and processes	Substrates	Age depositional environment
Aref (1998)	Interdependent morphotypes of microbial mats and associated lenticular gypsum	Siliciclastic, evaporitic	Holocene, East Egypt, coastal area, sabkha
Bernier et al. (1991)	Crescent, radial wavy, and lacerated structures, padded polygonal structures	Muddy carbonate, evaporite	Upper Jurassic, Kimmeridgian, Cerin, peritidal
Bruun-Petersen & Krumbein (1975)	Ripple marks, mud cracks, calcareous thin layers, evaporites	Mixed siliciclastic carbonate	Lower Triassic, Middle Buntsandstein, coastal area
Chafetz et al. (1993)	Black microbialites, calcified evaporite crystals. Ministromatolites, similar to the 'rugose surface of growing subaerial algal tufa' (Warren, 1982). Allochems (coated grains, pellets, rip-up clasts)	Mixed evaporitic carbonate	Upper Carboniferous, New Mexico, arid, paralic to shallow marine settings
Coleman & Raiswell (1993)	Microbial mineralization of organic matter	Clay, silt	Cretaceous
Davis (1968)	Siliciclastic stromatolites, laminated structures, ooids, intraclasts, dolomite USA	Sand, shale	Lower Ordovician, Minnesota
Dill & Kemper (1990)	Pyrite linked to biogenic hollows (burrows, tests), bedding planes, shrinkage cracks	Claystone, marl	Lower Cretaceous, Upper Barremian to Lower Aptian
Gautier (1982)	Siderite concretions, early diagenesis	Shale	Cretaceous
Gehling, 1991	Wrinkled bedding surfaces, cohesive sand laminae, rip-up clasts, syneresis cracks, moulds, Ediacaran death masks	Siliciclastic Coarse-grained sand	Terminal Proterozoic, Ediacaran
Hagadorn & Bottjer (1997)	Wrinkle marks, Kinneyia ripples	Siliciclastic sand	Terminal Proterozoic, Ediacaran
Kendall et al. (1994)	Cements, coatings, crinkled surface overlying gypsum mush, surface polygons, halite crusts, algal polygons, cinder-like mammilated and tufted algal surface overlying carbonates, intertidal polygonal hardgrounds, coated cerithid molluscs	Mixed carbonate –siliciclastic –evaporitic	Holocene, Abu Dhabi, beachrocks compared with Permian, Triassic, Tertiary formations
Leinfelder (1985)	Calcification morphotypes, oncolites, condensed schizothrix filaments, tufts	Mixed carbonate/ siliciclastic	Upper Jurassic, Kimmeridgian?, Portugal
Martín & Braga (1993)	Siliciclastic-carbonate stromatolites, thrombolites, fenestrae, lamina in sandstone stromatolite: siliciclastic grains exceed 50% of rock volume. Intervening micrite interpreted as microbial	Mixed carbonate/ siliciclastic	Upper Miocene, SE Spain, marine, shelf, upper slope, deeper environments

Peryt (1994)	Nodular anhydrite, bedded anhydrite, laminated gypsum formation, nodules, 'eye' structures	Evaporitic shallow to deep water	Upper Permian, Zechstein
Pflüger & Gresse, 1996	Microbial sand chips	Siliciclastic	Proterozoic/Cambrian
Sánchez-Navas *et al.* (1998)	Formation of finely laminated clays and carbonate fluorapatite in stromatolites	Mixed carbonate/siliciclastic	Upper Jurassic, SW Spain, pelagic swell
Schieber (1989a,b, 1990)	Carbonaceous laminae/drapes of dolomitic clayey shale, laminae lenticular to wavy, bed surfaces pustular-wrinkled, laminae with mica enrichment and/or randomly oriented micas, curved-wrinkled impressions on bedding planes, uparched laminae near mud-cracks, (dolomite, ferroan carbonates, pyrite), intraclasts, carbonaceous flakes (all facies characters of microbial mat presence, similar to modern records)	Siliciclastic	Mid-Proterozoic Montana, USA, Belt basin, deep-water mudstones in a turbidite setting, lamina-specific distribution of early diagenetic minerals
Selg (1986)	Bioherms, biostromes	Clay/sand interlayers	Lower Cambrian SW Sardinia
Soudry & Weissbrod (1995)	Thrombolites, siliciclastic stromatolites, rip-up clasts, carbonate beds intercalated in sandstone and siltstone dolomitic bands (relic microbial fabrics), low content of siliciclastics (10–15%). Siliciclastic stromatolites in cross-stratified sandstone at top of the Timna succession, *Skolithos* burrows sequence	Carbonate, sandstone/siltstone interlayers	Cambrian, prograding tidal following early transgression, Southern Israel
Tribovillard *et al.* (1992)	Flat-laminated or undulating types of stromatolite nodules, microbial endoliths, carbonate spheres	Organic sediment/carbonate	Upper Jurassic, Kimmeridgian, French Jura, lagoonal
Wahab (1991)	Stromatolite mounds, irregular surfaces with tepee structures, gypsum mounds, algal mats encrusted by crystalline gypsum, crumbling anhydrite crust	Evaporitic	Holocene, sabkha, evaporitic

functions with microstructural characteristics of sediments in tidal positions. Noffke & Krumbein (1999) have already furthered this aspect in their study of microbial stabilization of sedimenatry surfaces at the Mellum site.

Moving from this more actualistic viewpoint to the rock record, an overview of definite, as well as still speculative, structures of microbial origin (Table 4) underlines the potential of many signatures already included in this catalogue to become fossilized and provide strong indicators of former tidal siliciclastic settings. Once again, signatures with a ubiquitous occurrence can be recognized and, in contrast, signatures with a small facies tolerance. The number of indicative structures, however, decreases in the rock record, and only a few microbial structural signatures can be used to characterize their former environmental conditions.

The type of structures surviving diagenetic alteration is not restricted to one kind of category within the catalogue. Fossil examples from all sections of the catalogue are documented, but it seems that laminations and mineralogical features are the best representatives of each environment in the fossil record. This might be a distorted conclusion, as sedimentary surface structures are usually less accessible to study in ancient sequences. However, it is expected that, in a revision of relevant settings (Table 4), additional palaeo-analogues of signatures in the catalogue can be recognized in some cases. This assumption can be supported by the fact that: (1) most of the recently dominant structure-mediating microbes have been abundant over hundreds of millions of years; and (2) for even longer, microbial physiological pathways have not changed.

Seen against the background of climate and hydrodynamic energy, this catalogue comprises two main types of coastal variation: one (Mellum Island) is controlled by macrotidal ranges, accompanied by hydroenergetic forces that exceed weather-controlled environmental factors, and facilitates tidal flooding and related sediment transport even into the supratidal sites of microbial growth; in the other (Tunisian coast), the hydrodynamic energy is low as a result of microtides, and climatic factors clearly dominate the physical forces that modulate the microbial textural fabrics.

CONCLUSIONS

The presented catalogue is at an intermediary stage. It is expected that further textural signa-tures of microbial activity will be recognized in siliciclastic depositional environments with different physicoenergetic characteristics and different climatic conditions. Regarding settings that are less suitable for microbial activity, such as those with higher hydrodynamic regimes or cold and dry climates, the boundaries and limitations of the presence of significant microbial signatures can be assessed. This more complete catalogue would serve as a serious tool for a microbiological-based facies diagnosis with a high-resolution power for siliciclastic settings.

Further improvement to the catalogue will probably result from studies that consider the mineral components and chemical variations caused by microbial processes. Combined textural and chemical information may provide multiple criteria and therefore even stronger evidence on facies-dependent microbial activity in siliciclastic settings all over the earth and throughout earth history.

ACKNOWLEDGEMENTS

GLOSSARY

baffling (Fig. 6D): a process in which filamentous cyanobacteria stretch upwards forming an organic 'comb' perpendicular to the mat surface. The trichome bundles standing upright create microzones of lower current velocity that aid the settlement of smaller grains (compare also binding and trapping).

binding (Fig. 6B, C and E): a process in which deposited allochthonous material becomes enclosed within the growing mat or biofilms. Binding is sometimes triggered by 'baffling' (compare also trapping).

biofilm: surface accumulations of cells immobilized at a substratum and commonly embedded in an organic polymer matrix of microbial origin (Characklis & Marshall, 1990).

biolaminations (Fig. 3A and B): intercalated sand and microbial mat layers depending on (i) the sedimentation rate, and (ii) the length of time of zero sedimentation the organisms have in which to produce and condense new biomass layers.

biostabilization (Fig. 7): microbially stabilized sedimentary surface layers. Biostabilized sediments behave differently to physical reworking compared with non-stabilized deposits (Noffke *et al.*, 1996). While non-stabilized siliciclastic sediments usually break up into their individual mineral components at relatively low current velocities, stabilized sediments resist erosional forces.

biovarvite (Fig. 3C and G): alternating couplets of laminae produced by different cyanobacterial morphotypes: ensheathed filamentous cyanobacteria that form condensed laminae of fibrillar meshwork; coccoid cyanobacteria excreting polymeric substances (EPS) produce laminae swollen by viscous slime. Reasons for the couplet formation are rhythmic (often seasonal) dominance changes in distinct microbial populations. Multilaminated rhythmites generally form without the aid of sedimentation (descriptions in Gerdes *et al.*, 1991).

cohesive sand layers (Fig. 3A): bedding planes stabilized by microbial films that include filamentous (e.g. *Oscillatoria* sp.) and/or coccoidal cyanobacteria (e.g. *Merismopedia* sp.). Individual sand grains bound together by microbial extracellular polymers resist erosion up to certain limits.

condensed fibrillar meshworks (Fig. 3B): complex texture built by ensheathed filamentous cyanobacteria (morphotype responsible for stromatolitic lamination).

erosional pockets: rounded depressions of about 10–50 cm diameter, margins sharp or gradational. Bottoms of the pockets are contoured by erosion ripples. Crests of ripples merge laterally with the non-eroded bed surface. Caused by partial erosion of cohesive sand layers as a result of tide- and wave-controlled hydrodynamics (descriptions in Reineck, 1979).

erosional remnants (Fig. 7A): topographic features, a few centimetres high, representing residual stacks of biolaminated build-ups left after destruction of the former biostabilized surface layer (detailed descriptions in Noffke, 1999).

EPS: extracellular polymer substances, an important cell surface component as well as being part of the biofilm structure (Neu, 1994). Consist of polysaccharides, glycoproteins, other complex molecules such as melanins and other pigments or refractory polymerized substances (Krumbein, 1994).

'frozen' structures (i.e. ripple marks, filaments): secondary consolidation of structures of different origins by subsequent biofilm formation. 'Frozen ripple marks' (Fig. 5C): ripple consolidation by subsequently invading biofilms, which stabilize the sand grains against further transport. 'Frozen filaments' (Fig. 9G): calcification of filamentous cyanobacteria in an upward position.

intrinsic biofactors: factors that are inherent in the microbial species, e.g. morphotypes and behaviour of mat-producing cyanobacteria. Cyanobacteria involved in structural diversification of biofilms and mats include ensheathed and 'naked' filamentous forms, encapsulated and 'naked' coccoidal forms and cells with both random dispersal and colonial aggregation. Internal and surface fabrics of mats also depend on the structural and induced polarity of species.

mat chips (Fig. 7C–F): organosedimentary fragments of biostabilized sediments. Types of mat chips are distinguished according to form, sediment content and transport behaviour.

microbial biostrome (Fig. 3B): sheet-like microbial biomass overgrowing the sediment surface. Often in a multilaminated pattern. Basic area: principally wider than the height of the build-up (in contrast, other biological build-ups project significantly above the sediment surface in dimensions higher than the width of the basic area).

microbial mat: microfibrous, slime-interwoven, coherent coatings of sedimentary and other surfaces, which, by their morphology, physiology, and arrangement in space and time, interact with the physical and chemical environment to produce a laminated pattern (Krumbein, 1983).

petees (Fig. 8A–D): domes or folds in surface layers stabilized by biogenic matrices, with rounded crests and a vertical section like an inverted 'U'. In arid settings, crests are often ruptured, and limbs of folds partially overthrust (detailed description in Reineck *et al.*, 1990).

pinnacles, tufts (Fig. 3C): products of polarity changes in filamentous cyanobacteria originally contributing to condensed fibrillar meshworks. Erected filament bundles rise some millimetres above mat base. Often embedded in EPS.

polarity: the spatial orientation of mat-forming benthic cyanobacteria is of great importance for the type of mat produced. Basically, the preferential spatial orientation of filamentous cyanobacteria (and others) is a result of their polar attributes. Two possible pathways exist (Scholz, 1996): a growth direction that is causal

to the cell (cytoplasma) organization and taxon-specific division planes, which is termed 'structural polarity'; growth directions induced by ecological factors (e.g. light, gravitation) are termed 'induced polarity'.

sinoidal laminae (Fig. 5A): organic coatings of troughs and lee faces of ripples by biofilms and mats as an ecological response of the constituting organisms to ripple formation. Organisms respond ecologically to the irregular surface topography, settling preferentially in the ripple troughs and on the lee faces.

sponge pore fabrics (Fig. 9A and B): hollow pores of 0·5–3 mm in diameter arranged like pearl strings in sandy interlayers between organic laminae, representing records of gas diffusion in biostabilized sediments. Regular distribution of pores indicating that sponge fabrics are maintained by buried mats and biofilms (detailed description in Noffke *et al.*, 1997b).

taxis: movement of organisms initiated by a stimulus.

thrombolitic fabrics (Fig. 4C): unlaminated to poorly laminated loaf- to mound-shaped structures with a macroscopic clotted fabric. Dominance of coccoid cyanobacteria producing amounts of EPS.

trapping (Fig. 3A): a process that glues particles to the sticky mat surface (compare also binding).

REFERENCES

Allison, P.A. (1988) The role of anoxia in the decay and mineralization of proteinaceous macro-fossils. *Paleobiology*, **14**, 139–154.

Aref, M.A.M. (1998) Holocene stromatolites and microbial laminites associated with lenticular gypsum in a marine-dominated environment, Ras El Shetan, Gulf of Aqaba, Egypt. *Sedimentology*, **45**, 245–256.

Bauld, J. (1984) Microbial mats in marginal marine environments: Shark Bay, Western Australia, and Spencer Gulf, South Australia. In: *Microbial Mats: Stromatolites* (Eds Y. Cohen, R.W. Castenholz and H.O. Halvorson), pp. 39–58. Liss, New York.

Bernier, P., Gaillard, C., Gall, J.C., Barale, G., Bourseau, J.P., Buffetaut, E. and Wenz, S. (1991) Morphogenetic impact of microbial mats on surface structures of Kimmeridgian micritic limestones (Cerin, France). *Sedimentology*, **38**, 127–136.

Bruun-Petersen, J. and Krumbein, W.E. (1975) Rippelmarken, Trockenrisse und andere Seichtwassermerkmale im Buntsandstein von Helgoland. *Geol. Rundsch.*, **64**, 126–143.

Chafetz, H.S. and Buczynski, C. (1992) Bacterially induced lithification of microbial mats. *Palaios*, **7**, 277–293.

Chafetz, H.S., Rush, P.F. and Schoderbek, D. (1993) Occult aragonitic fabrics and structures within microbiolites, Pennsylvanian Panther Seep Formation, San Andres Mountains, New Mexico, USA. *Carbonates Evaporites*, **8**, 123–134.

Characklis, W.G. and Marshall, K.C. (eds) (1990) *Biofilms.* Wiley, New York.

Coleman, M.L. and Raiswell, R. (1993) Microbial mineralization of organic matter: mechanisms of self-organization and inferred rates of precipitation of diagenetic minerals. *Phil. Trans. R. Soc. London A*, **344**, 69–87.

Dahanayake, K. and Krumbein, W.E. (1986) Microbial structures in oolitic iron formations. *Mineral. Deposita*, **21**, 85–94.

Davaud, E. and Septfontaine, M. (1995) Post-mortem onshore transportation of epiphytic foraminifera: recent example from the Tunisian coastline. *J. Sedim. Res.*, **A65**, 136–142.

Davis, R.A. Jr (1968) Algal stromatolites composed of quartz sandstone. *J. Sedim. Petrol.*, **38**, 953–955.

Dill, H. and Kemper, E. (1990) Crystallographic and chemical variations during pyritization in the upper Barremian and lower Aptian dark claystones from the Lower Saxonian Basin (NW Germany). *Sedimentology*, **37**, 427–443.

Friedman, G.M., Sanders, J.E. and Kopaska-Merkel, D. (1992) *Principles of Sedimentary Deposits.* Macmillan, New York.

Führböter, A. and Manzenrieder, H. (1987) Biostabilisierung von Sandwatten durch Mikroorganismen. In: *Mellum, Portrait einer Insel* (Eds G. Gerdes, W.E. Krumbein and H.E. Reineck), pp. 123–138. Kramer, Frankfurt am Main.

Gautier, D.L. (1982) Siderite concretions: indicators of early diagenesis in the Gammon Shale (Cretaceous). *J. Sedim. Petrol.*, **52**, 859–871.

Gehling, J.G. (1991) The case for Ediacaran fossil roots to the metazoan tree. *Geol. Soc. India Mem.*, **20**, 181–224.

Geitler, L. (1932) Cyanophyceae. In: *Kryptogamenflora von Deutschland, Österreich und der Schweiz*, Vol. 14 (Ed. L. Rabenhorst), Akad. Verlagsges, Leipzig.

Gerdes, G. and Krumbein, W.E. (1987) Biolaminated deposits. In: *Lecture Notes in Earth Sciences 9* (Eds S. Bhattacharya, G.M. Friedman, H.J. Neugebauer and A. Seilacher), pp. 1–183. Springer, Berlin.

Gerdes, G. and Reineck, H.E. (1987) Aktuogeologie und Aktuopaläontologie des Farbstreifen-Sandwattes von Mellum. In: *Mellum, Portrait Einer Insel* (Eds G. Gerdes, W.E. Krumbein and H.E. Reineck), pp. 219–233. Kramer, Frankfurt am Main.

Gerdes, G., Krumbein, W.E. and Reineck, H.E. (1991) Biolaminations – ecological versus depositional dynamics. In: *Cycles and Events in Stratigraphy* (Eds G. Einsele, W. Ricken and A. Seilacher), pp. 592–607. Springer, Berlin.

Gerdes, G., Claes, M., Dunajtschik-Piewak, K., Riege, H., Krumbein, W.E. and Reineck, H.E. (1993) Contribution of microbial mats to sedimentary surface structures. *Facies*, **29**, 61–74.

Gerdes, G., Krumbein, W.E. and Reineck, H.E. (1994a) Microbial mats as architects of sedimentary surface structures. In: *Biostabilization of Sediments* (Eds W.E. Krumbein, D.M. Paterson and L.J. Stal), pp. 165–182. BIS, Oldenburg.

Gerdes, G., Dunajtschik-Piewak, K., Riege, H., Taher, A.G., Krumbein, W.E. and Reineck, H.E. (1994b) Structural diversity of biogenic carbonate particles in microbial mats. *Sedimentology*, **41**, 1273–1294.

Golubic, S. and Knoll, A.H. (1993) Prokaryotes. In: *Fossil Prokaryotes and Protists* (Ed. J.H. Lipps), pp. 51–76. Blackwell Science, Oxford.

Guerrero, R. and Mas, J. (1989) Multilayered microbial communities in aquatic ecosystems: Growth and loss factors. In: *Microbial Mats, Physiological Ecology of Benthic Microbial Communities* (Eds Y. Cohen and E. Rosenberg), pp. 37–51. American Society of Microbiology, Washington, DC.

Hagadorn, J.W. and Bottjer, D.J. (1997) Wrinkle structures: microbially mediated sedimentary structures common in subtidal siliciclastic settings at the Proterozoic-Phanerozoic transition. *Geology*, **25**, 1047–1050.

Javor, B. and Castenholz, R.W. (1984) Productivity studies of microbial mats, Laguna Guerrero Negro, Mexico. In: *Microbial Mats: Stromatolites* (Eds Y. Cohen, R.W. Castenholz and H.O. Halvorson), pp. 149–170. Liss, New York.

Kendall, C.G. St C., Sadd, J.L. and Alshartian, A. (1994) Holocene marine cement coatings on beach-rocks of the Abu Dhabi coastline (UAE); Analogs for cement fabrics in ancient limestones. *Carbonates Evaporites*, **9**, 119–131.

Kropp, J., Block, A., von Bloh, W., Klenke, Th. and Schellnhuber, H.J. (1997) Multifractal characterization of microbially induced calcite formation in Recent tidal flat sediments. *Sedim. Geol.*, **109**, 37–52.

Krumbein, W.E. (1974) On the precipitation of aragonite on the surface of marine bacteria. *Naturwissenschaft*, **61**, 167.

Krumbein, W.E. (1983) Stromatolites – the challenge of a term in space and time. *Precambrian Res.*, **20**, 493–531.

Krumbein, W.E. (1994) The year of the slime. In: *Biostabilization of Sediments* (Eds W.E. Krumbein, D.M. Paterson and L.J. Stal), pp. 1–7. BIS, Oldenburg.

Leinfelder, R.R. (1985) Cyanophyte calcification morphotypes and depositional environments (Alenquer Oncolite, Upper Kimmeridigan?, Portugal). *Facies*, **12**, 253–274.

MacKenzie, D.B. (1968) Studies for students: Sedimentary features of Alameda Avenue cut, Denver, Colorado. *Mountain Geologist*, **5**, 3–13.

Martín, J.M. and Braga, J.C. (1993) Siliciclastic stromatolites and thrombolites, Late Miocene, SE Spain. *J. Sedim. Petrol.*, **63**, 131–139.

Monty, C.L.V. (1976) The origin and development of cryptalgal fabrics. In: *Stromatolites* (Ed. M.R. Walter), pp. 193–243. Elsevier, Amsterdam.

Neu, T.R. (1994) Biofilms and microbial mats. In: *Biostabilization of Sediments* (Eds W.E. Krumbein, D.M. Paterson and L.J. Stal), pp. 9–16. BIS, Oldenburg.

Noffke, N. (1997) *Mikrobiell Induzierte Sedimentstrukturen (M.I.S.S.) in Siliziklastischen Wattsedimenten.* Doctoral Thesis, University of Oldenburg, Oldenburg.

Noffke, N. (1998) Multidirected ripple marks rising from biological and sedimentological processes in modern lower supratidal deposits (Mellum Island, southern North Sea). *Geology*, **26**, 879–892.

Noffke, N. (1999) Erosional remnants and pockets evolving from biotic–physical interactions in a Recent lower supratidal environment. *Sedim. Geol.*, **123**, 175–181.

Noffke, N. and Krumbein, W.E. (1999) A quantitative approach to sedimentary surface structures contoured by the interplay of microbial colonization and physical dynamics. *Sedimentology*, **46**, 417–426.

Noffke, N., Gerdes, G., Klenke, Th. and Krumbein, W.E. (1996) Microbially induced sedimentary structures – Examples from modern siliciclastic tidal flat sediments. *Zentralbl. Geol. Paläont. I*, **1995** (1/2), 307–316.

Noffke, N., Gerdes, G., Klenke, Th. and Krumbein, W.E. (1997a) A microscopic sedimentary succession indicating the presence of microbial mats in siliciclastic tidal flats. *Sedim. Geol.*, **110**, 1–6.

Noffke, N., Gerdes, G., Klenke, Th. and Krumbein, W.E. (1997b) Biofilm impact on sedimentary structures in siliciclastic tidal flats. *Cour. Forsch.-Inst. Senckenberg*, **201**, 297–305.

Peryt, T. (1994) The anatomy of a sulphate platform and adjacent basin system in the Leba sub-basin of the Lower Werra Anhydrite (Zechstein, Upper Permian), northern Poland. *Sedimentology*, **41**, 83–113.

Pflüger, F. and Gresse, P.G. (1996) Microbial sand chips – a non-actualistic sedimentary structure. *Sedim. Geol.*, **102**, 263–274.

Reineck, H.E. (1970) Reliefguß und projizierbarer Dickschliff. *Senck. Marit.*, **2**, 61–66.

Reineck, H.E. (1979) Rezente und fossile Algenmatten und Wurzelhorizonte. *Natur Museum*, **109**, 290–296.

Reineck, H.E., Gerdes, G., Claes, M., Dunajtschik, K., Riege, H. and Krumbein, W.E. (1990) Microbial modification of sedimentary surface structures. In: *Sediments and Environmental Geochemistry* (Eds D. Heling, P. Rothe, U. Förstner and P. Stoffers), pp. 254–276. Springer, Berlin.

Riding, R. (1991) Classification of microbial carbonates. In: *Calcareous Algae and Stromatolites* (Ed. R. Riding), pp. 21–51. Springer, Berlin.

Riege, H. (1991) Contribution of heterotrophic bacteria to the formation of $CaCO_3$-aggregates in hypersaline microbial mats. *Kieler Meeresforsch.*, **8**, 168–172.

Rippka, R., Deruelles, J., Waterbury, J.B., Herdman, M. and Stanier, R.Y. (1979) Generic assignments, strain histories and properties of pure cultures of cyanobacteria. *J. Gen. Microbiol.*, **111**, 1–61.

Sánchez-Navas, A., Martín-Algarra, A. and Nieto, F. (1998) Bacterially-mediated authigenesis of clays in phosphate stromatolites. *Sedimentology*, **45**, 519–533.

Schieber, J. (1989a) Facies and origin of shales from the mid-Proterozoic Newland Formation, Belt basin, Montana, USA. *Sedimentology*, **36**, 203–219.

Schieber, J. (1989b) Pyrite mineralization in microbial mats from the mid-Proterozoic Newland Formation, Belt Supergroup, Montana, USA. *Sedim. Geol.*, **64**, 79–90.

Schieber, J. (1990) Significance of styles of epicontinental shale sedimentation in the Belt basin, mid-Proterozoic of Montana, USA. *Sedim. Geol.*, **69**, 297–312.

Scholz, J. (1996) *Eine Feldtheorie der Bryozoen, Mikrobenmatten und Sedimentoberflächen.* Habilitationsschrift, Universität Hamburg.

Schulz, E. (1937) Das Farbstreifen-Sandwatt und seine Fauna, eine ökologisch-biozönotische Untersuchung an der Nordsee. *Meereskundl. Arb. Univ. Kiel*, **1**, 359–378.

Selg, M. (1986) Algen als Faziesindikatoren: Bioherme und Biostrome im Unter-Kambrium von SW-Sardinien. *Geol. Rundschau*, **75**, 693–702.

Shinn, E.A. (1972) Worm and algal-built columnar stromatolites in the Persian Gulf. *J. Sedim. Petrol.*, **42**, 837–840.

Skyring, G.W. and Bauld, J. (1990) Microbial mats in Australian coastal environments. In: *Advances in Microbial Ecology 11* (Ed. K.C. Marshall), pp. 461–498. Plenum, New York.

Soudry, D. and Weissbrod, T. (1995) Morphogenesis and facies relationships of thrombolites and siliciclastic stromatolites in a Cambrian tidal sequence (Elat area, southern Israel). *Palaeogeogr., Palaeoclimatol., Palaeoecol.*, **114**, 339–355.

Stal, L.J. and Krumbein, W.E. (1985) Isolation and characterization of cyanobacteria from a marine microbial mat. *Bot. Mar.*, **28**, 351–365.

Tribovillard, N.P., Gorin, G.E., Belin, S., Hopfgarnter, G. and Pichon, R. (1992) Organic-rich biolaminated facies from a Kimmeridigan lagoonal environment in the French Southern Jura mountains – A way of estimating accumulation rate variations. *Palaeogeogr., Palaeoclimatol., Palaeoecol.*, **99**, 163–177.

Wachendörfer, V. (1991) The fluorescent sediment thin section technique: spatial distribution of microorganisms in North Sea microbial mat systems. *Helgol. Meeresforsch.*, **8**, 381–388.

Wahab, S.A. (1991) Ras Shukeir sabkha and associated salina deposits: Comparison with a Holocene depositional equivalent. *Carbonates Evaporites*, **6**, 1–12.

Warren, J.K. (1982) The hydrological significance of Holocene tepees, stromatolites and boxwork limestones in coastal salinas in south Australia. *J. Sedim. Petrol.*, **52**, 1171–1201.